Brain Research 1719 (2019) 157–175

Contents lists available at ScienceDirect

Brain Research

journal homepage: www.elsevier.com/locate/brainres

Research report

Methamphetamine persistently increases alpha-synuclein and suppresses gene promoter methylation within striatal neurons

Francesca Biagioni[a,1], Rosangela Ferese[a,1], Fiona Limanaqi[b], Michele Madonna[a], Paola Lenzi[b], Stefano Gambardella[a], Francesco Fornai[a,b,*]

[a] I.R.C.C.S. I.N.M. Neuromed, via Atinense 18, 86077 Pozzilli (IS), Italy
[b] Department of Translational Research and New Technologies in Medicine and Surgery, University of Pisa, via Roma 55, 56126 Pisa, Italy

HIGHLIGHTS

- Methamphetamine persistently reduces nigrostriatal DA innervation.
- Methamphetamine persistently increases striatal alpha synuclein.
- Methamphetamine does not alter synuclein gene sequence and copy number.
- Methamphetamine depresses methylation within alpha synuclein gene promoter.
- Methamphetamine-induced toxicity and epigenetic stimulation of *SNCA* do not overlap.

ARTICLE INFO

Keywords:
Methamphetamine
Alpha-synuclein
Hypomethylation
SNCA promoter
Epigenetics of drug abuse
Transmission electron microscopy

ABSTRACT

Methamphetamine (Meth) produces a variety of epigenetic effects in the brain, which are seminal to establish long-lasting alterations in neuronal activity. However, most epigenetic changes were described by measuring the rough amount of either histone acetylation and methylation or direct DNA methylation, without focusing on a specific DNA sequence. This point is key to comprehend Meth-induced phenotypic changes, brain plasticity, addiction and neurodegeneration. In this research paper we analyze the persistence of Meth-induced striatal synucleinopathy at a prolonged time interval of Meth withdrawal. At the same time, Meth-induced alterations, specifically within alpha-synuclein gene (*SNCA*) or its promoter, were evaluated. We found that exposure to high and/or prolonged doses of Meth, apart from producing nigro-striatal toxicity, determines a long-lasting increase in striatal alpha-synuclein levels. This is consistent along immune-blotting, immune-histochemistry, and electron microscopy. This was neither associated with an increase of *SNCA* copy number nor with alterations within *SNCA* sequence. However, we documented persistently demethylation within *SNCA* promoter, which matches the increase in alpha-synuclein protein. The amount of the native protein, which was measured stoichiometrically within striatal neurons, surpasses the increase reported following *SNCA* multiplications. Demethylation was remarkable (ten-fold of controls) and steady, even at prolonged time intervals being tested so far (up to 21 days of Meth withdrawal). Similarly alpha-synuclein protein assayed stoichiometrically steadily increased roughly ten-fold of controls. Meth-induced increase of alpha-synuclein was also described within limbic areas. These findings are discussed in the light of Meth-induced epigenetic changes, Meth-induced phenotype alterations, and Meth-induced neurodegeneration.

1. Introduction

Methamphetamine (Meth) administration leads to experimental parkinsonism in rodents (Wagner et al., 1979, 1980a,b; Ricaurte et al., 1980, 1982; Wagner et al., 1983; Ricaurte et al., 1984; Seiden, 1985; Cadet et al., 2010; Smith et al., 2012; Kousik et al., 2014; McConnell

* Corresponding author at: I.R.C.C.S Neuromed, via Atinense 18, 86077 Pozzilli (IS), Italy, and Department of Translational Research and New Technologies in Medicine and Surgery, University of Pisa, via Roma 55, 56126 Pisa, Italy.
E-mail addresses: francesca.biagioni@neuromed.it (F. Biagioni), ferese.rosangela@gmail.com (R. Ferese), f.limanaqi@studenti.unipi.it (F. Limanaqi), mikelemadonna@yahoo.it (M. Madonna), paola.lenzi@med.unipi.it (P. Lenzi), stefano.gambardella@neuromed.it (S. Gambardella), francesco.fornai@neuromed.it, francesco.fornai@med.unipi.it (F. Fornai).
[1] These authors equally contributed to the present manuscript.

https://doi.org/10.1016/j.brainres.2019.05.035
Received 30 April 2019; Received in revised form 24 May 2019; Accepted 27 May 2019
Available online 28 May 2019

et al., 2015) and primates (Seiden et al., 1976; Seiden 1985; Preston et al., 1985; Woolverton et al., 1989; Villemagne et al., 1998, 1999; Kowall et al., 2000; Aubert et al., 2005), while in humans long-lasting Meth intake may increase the risk to develop Parkinson's disease (PD) (Volkow et al., 2001; Callaghan et al, 2012).

PD is included in a disease group named synucleinopathies (Galvin et al., 1999; McCormack and Di Monte, 2009). In fact, apart from rare PD phenotypes (Doherty et al., 2013) the occurrence of alpha-synuclein (α-syn) aggregates is a hallmark of such a disorder (Baba et al., 1998; Spillantini et al., 1998; Campbell et al., 2000; Iseki et al., 2000; Irvine et al., 2008; Goedert et al., 2010; Lee et al., 2010; Wong and Krainc, 2017; Melki, 2018). This occurs in sporadic and mostly genetic PD. In turn, mutations in the gene coding for α-syn (*SNCA*) are associated with genetic, dominantly inherited PD (Nussbaum and Polymeropoulos, 1997; Gasser, 1998; Spacey and Wood, 1999; Hardy et al., 2006; Gasser, 2007; Mizuno et al., 2008; Singleton et al., 2013; Koros et al., 2017), which suggests a detrimental gain of function of α-syn. In line with this, *SNCA* multiplications lead to familial PD (Singleton et al., 2003, 2013; Farrer et al., 2004; Ferese et al., 2015), where α-syn is overexpressed but its amino-acid sequence is intact and PD phenotype varies, being often severe (Kiely et al., 2015).

Such evidence strengthens the concept that a gain of function of α-syn (either due to altered conformation or an excess amount of normally conformed protein) drives molecular events leading to brain alterations. These data suggest that environmental factors, including drugs, when able to increase persistently the expression of *SNCA* may foster the occurrence of a synucleinopathy.

In fact, a previous study demonstrated that repeated Meth administrations lead to increased expression of α-syn in the *substantia nigra*, suggesting that environmental factors, including drugs, may predispose to PD (Fornai et al., 2005a). In fact, in sporadic PD patients, an epigenetic activation of intron1 in the *SNCA* promoter region may take place (Matsumoto et al., 2010).

Meth administration produces a powerful DA release, which affects post-synaptic neurons. In fact, high doses of Meth produce striatum-driven motor stereotypies, since striatal neurons are affected indeed by Meth administration (Zhu et al., 2006; Lazzeri et al., 2007; Cadet et al., 2013; Limanaqi et al., 2018). At the same time, due to a powerful connection between nigro-striatal TH positive and intrinsic striatal neurons, joined with a high propensity of α-syn to propagate along anatomically connected regions (Desplats et al., 2009; Olanow and Prusiner, 2009), it is likely that Meth-induced α-syn overexpression may recruit the post-synaptic site. Remarkably, the spreading of α-syn is fostered by overexpression of α-syn itself within target neurons (Thakur et al., 2017). Again, D1-like DA receptors are involved in Meth-induced accumulation of α-syn within striatal neurons (Lazzeri et al., 2007). This is demonstrated by preventing Meth-induced synucleinopathy by pre-treating mice with D1-like DA receptor antagonists or reproducing α-syn accumulation by administering D1-like DA receptor agonists dose-dependently *in vivo* or *in vitro* within mouse striatum or primary striatal cell cultures, respectively (Lazzeri et al., 2007), or even by administering DA to cell lines (Matsumoto et al., 2010). More recently, these effects were confirmed within hippocampal neurons, which accumulate α-syn following D1-like receptor agonists (Reichenbach et al., 2015). This is consistent with a number of studies showing the recruitment of non-canonical D1-like receptor signaling in the epigenetic effects which take place both in Meth-addicted and PD brains (Aubert et al., 2005; Guigoni et al., 2005, 2007; Biagioni et al., 2009; Berthet et al., 2009, 2012; Fornai et al., 2009; Barroso-Chinea et al., 2015; Li et al., 2015). In the present study, we used various treatment protocols aimed at assessing the amount and persistence of Meth-induced increase in α-syn. In addition, the effects of Meth administration at different dosing and following different time intervals were analyzed at genetic level. Since amphetamines alter DNA stability by inducing long tails in the comet assay (Frenzilli et al., 2006, 2007), we sought to comprehend whether Meth-induced alterations of striatal α-syn may depend on striatal DNA alterations. Therefore, we analyzed whether Meth induces DNA point mutations leading to a PARK1-like genotype or a gene multiplication (as it occurs in the PARK4 genotype). Finally, considering the amount of epigenetic effects produced by Meth (Zhu et al., 2006; Renthal and Nestler 2008; Cadet et al., 2010, 2013; Robison and Nestler 2011; Omonijo et al., 2014; Godino et al., 2015; Li et al., 2015; Massart et al., 2015; Walker and Nestler 2018; Limanaqi et al., 2018), we investigated *ex vivo*, within the mouse striatum, whether an activation in the promoter region of *SNCA* was generated by these protocols of Meth administration. Therefore, we analyzed the potential time-course and dosing-dependency of CpG islands demethylation within *SNCA* promoter.

In fact, it was crucial to understand whether a reiterated Meth exposure, among a variety of epigenetic effects (Omonijo et al., 2014), might specifically generate an up-regulation of *SNCA*, persisting for weeks of Meth withdrawal. Again, since we detected indeed a long-lasting increase in striatal-syn by immune-blotting and immune-histochemistry (which could not reliably detect neuronal compartmentalization), we further applied ultrastructural morphometry of intrinsic striatal neurons. Within these cells, we could also measure in situ the stoichiometric amount of α-syn molecules by immune-gold transmission electron microscopy. Experimental protocols encompass acute and prolonged Meth administrations, where the effects of Meth on striatal α-syn expression were matched with a rough assay of nigro-striatal toxicity.

2. Results

2.1. Meth reduces tyrosine-hydroxylase immune-staining in the acute time-course protocol

Immune-blot analysis (Fig. 2A, left item) shows that administration of Meth (5 mg/Kg × 5, 2 h apart) in a single day, does not modify striatal TH levels at 1 h but produces a moderate TH loss at 24 h and 7d following administration. Densitometric analysis (Fig. 2A, right item) indicates that such a dose of Meth reduces the level of the TH protein to roughly a half of Controls at 24 h and 7 d. TH immune-histochemistry substantiates the decrease of TH immune-reactivity within the dorsal striatum, at 24 h and 7 d after Meth administration. In Fig. 2B, left panel, the representative pictures show intense TH immune-staining both in Control and at 1 h after Meth. In contrast, pale TH immune-staining is visualized at 24 h and 7 d following Meth administration. When the density of TH immune-staining was quantified in the graph of Fig. 2B, right panel, the numerical values confirm almost a half reduction of striatal TH immune-staining at 24 h and 7 d following Meth, while at 1 h after Meth the staining is similar to Controls.

2.2. Meth reduces tyrosine-hydroxylase immune-staining following both sub-acute and chronic time-course protocols

Fig. 3A, left item shows representative SDS-PAGE immune-blotting of TH from saline and Meth-administered mice according to the sub-acute (5 mg/kg × 7d) or chronic (5 mg/kg × 21 d) protocol. In both protocols, the time-course was carried out at 24 h, 7 d, and 21 d after the last Meth injection. Representative blots show a decrease in the TH spot, which is similar for all time intervals following Meth administration (24 h, 7d and 21d) according to the sub-acute time-course protocol (daily administration of Meth 5 mg/kg × 7d). In the right lanes of the blot, the effects of a prolonged (21 d) daily Meth administration (chronic time-course protocol) produced a similar decrease in TH density, independently of the time interval of Meth withdrawal. This indicates that TH loss induced by Meth persists at 21 d of Meth withdrawal following a mild (5 mg/kg × 7 d) daily dose of Meth. This occurs even when such a daily dose is administered only for 7 d. In fact, as shown in the graph of Fig. 3A, prolonging Meth administration up to 21 d does not further decrease striatal TH levels detected at SDS-PAGE

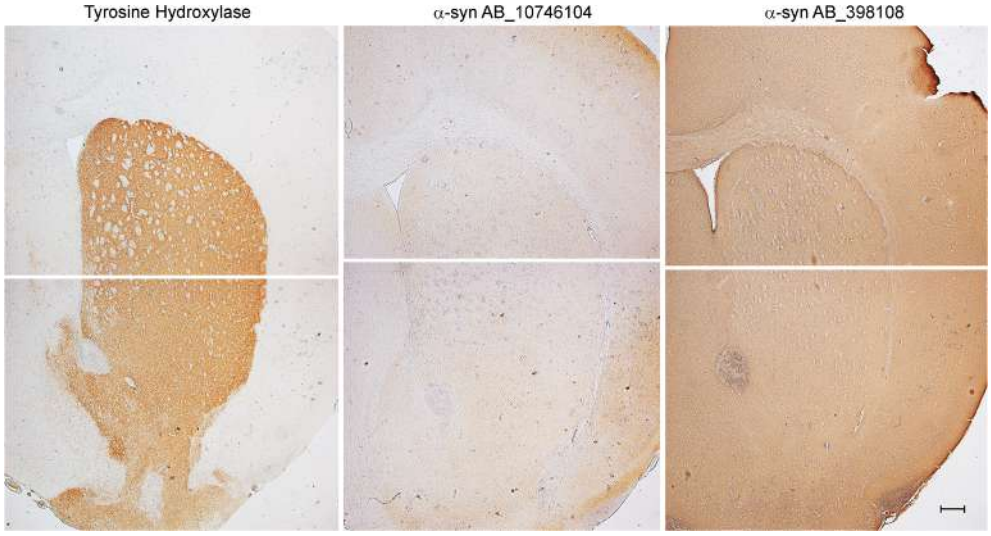

Fig. 1. Pilot dual alpha-synuclein-immune-staining compared with classic tyrosine-hydroxylase-immune-staining in the whole striatum. Slices from Controls (saline-treated mice) at striatal level (AP = +1.10 from Bregma) were stained to show representative images of differential α-syn immune-staining depending on different primary antibody and tissue processing. In this pilot study striatal α-syn immune-staining with Sigma Aldrich antibody (AB_10746104; middle slice) was compared with a currently available BD anti-α-syn-antibody (AB_398108; right slice); the left slice reports a classic striatal TH immune-staining (Sigma Aldrich; AB_477560; left slice). Immune-staining with anti-α-syn-antibody shows a higher specificity for Sigma compared with BD anti-α-syn-antibody. This staining is comparable with that obtained using the α90 antibody both for immune-histochemistry and immune-cyto-chemistry (Totterdell et al., 2004) and it was quite similar to total α-syn (AB_52168; 1:200 in BSA 1% PBST; Abcam, Cambridge, UK), used by Novello et al. (2018) or human anti-α-syn (AB_36615, 1:1000, Abcam, UK) as used by Mulcahi et al. (2006). Scale bar 200 μm.

immune-blotting. On the other hand, these data indicate that Meth is neurotoxic even when it is administered in single slight doses (5 mg/kg) for a week. In Fig. 3B left item, representative pictures of striatal TH-immune-staining, at different time intervals, following a sub-acute Meth administration are shown. These pictures provide indirect evidence for a decrease in nigro-striatal DA innervation, at 24 h, 7 d and 21 d following a week of 5 mg/Kg daily Meth administration. These representative pictures are backed by values reported in the graph of Fig. 3B. It is worth mentioning that following this protocol of Meth administration, at 7 d of withdrawal there is a further decrease of TH levels compared with the loss measured at 24 h. Remarkably, at prolonged time intervals of Meth withdrawal (21 d) a significant recovery of striatal TH occurs compared with the TH loss which was measured both at 24 h and at 7 d. This recovery is partial since TH levels at 21 d of withdrawal remain significantly lower than Controls. Similar results were obtained for the same time intervals, following a prolonged daily

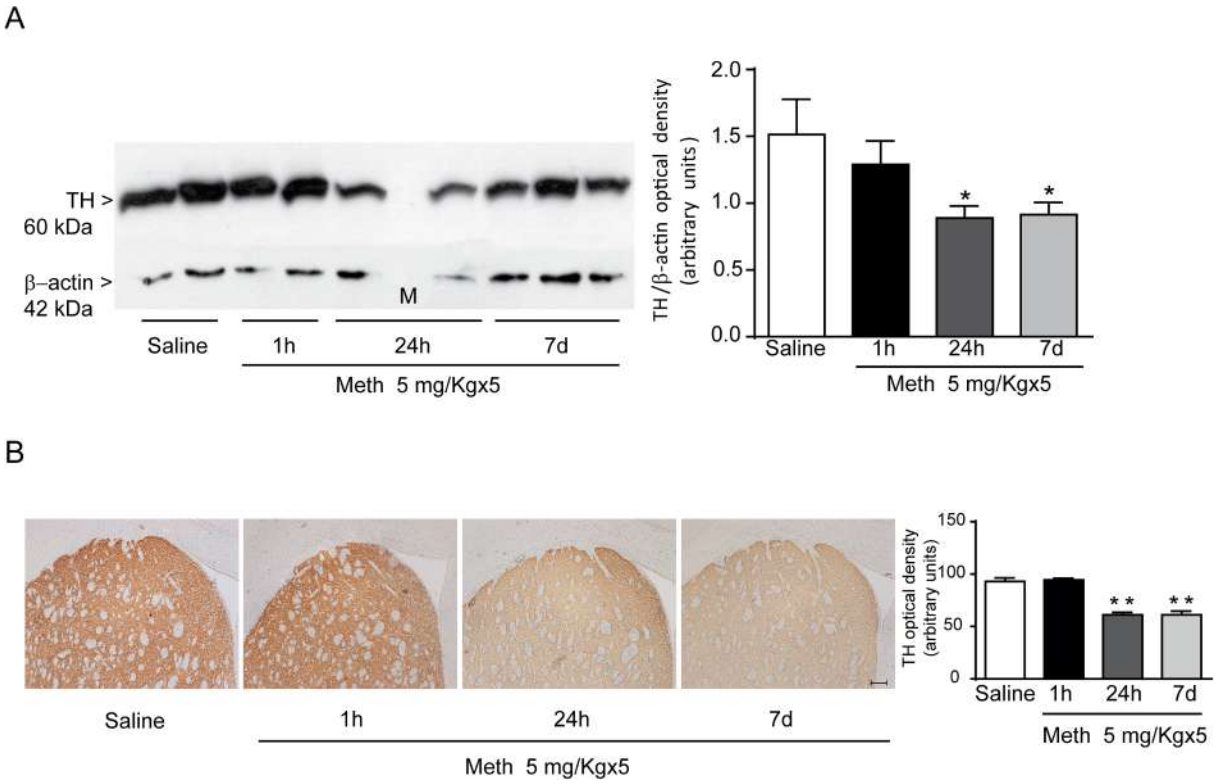

Fig. 2. Methamphetamine reduces tyrosine-hydroxylase immune-reactivity in the acute time-course protocol. In panel **A**, immune-blot analysis shows a significant reduction in TH protein levels at 24 h and 7d after the last Meth administration according to the acute time-course protocol (5 mg/Kg × 5, 2 h apart). No changes were detected at 1 h (left and right panel) (*$p = 0.0052$ *vs.* saline alone). In panel **B**, immune-histochemical analysis of TH expression confirm the data obtained from immune-blot analysis at the times analyzed. Densitometric analysis ratifies the data obtained in the striatum of Meth-treated animals compared with Controls (saline-treated mice, Fig. 1B, right panel) (**$p < 0.0001$ *vs.* saline and Meth 1 h). Scale bar 100 μm.

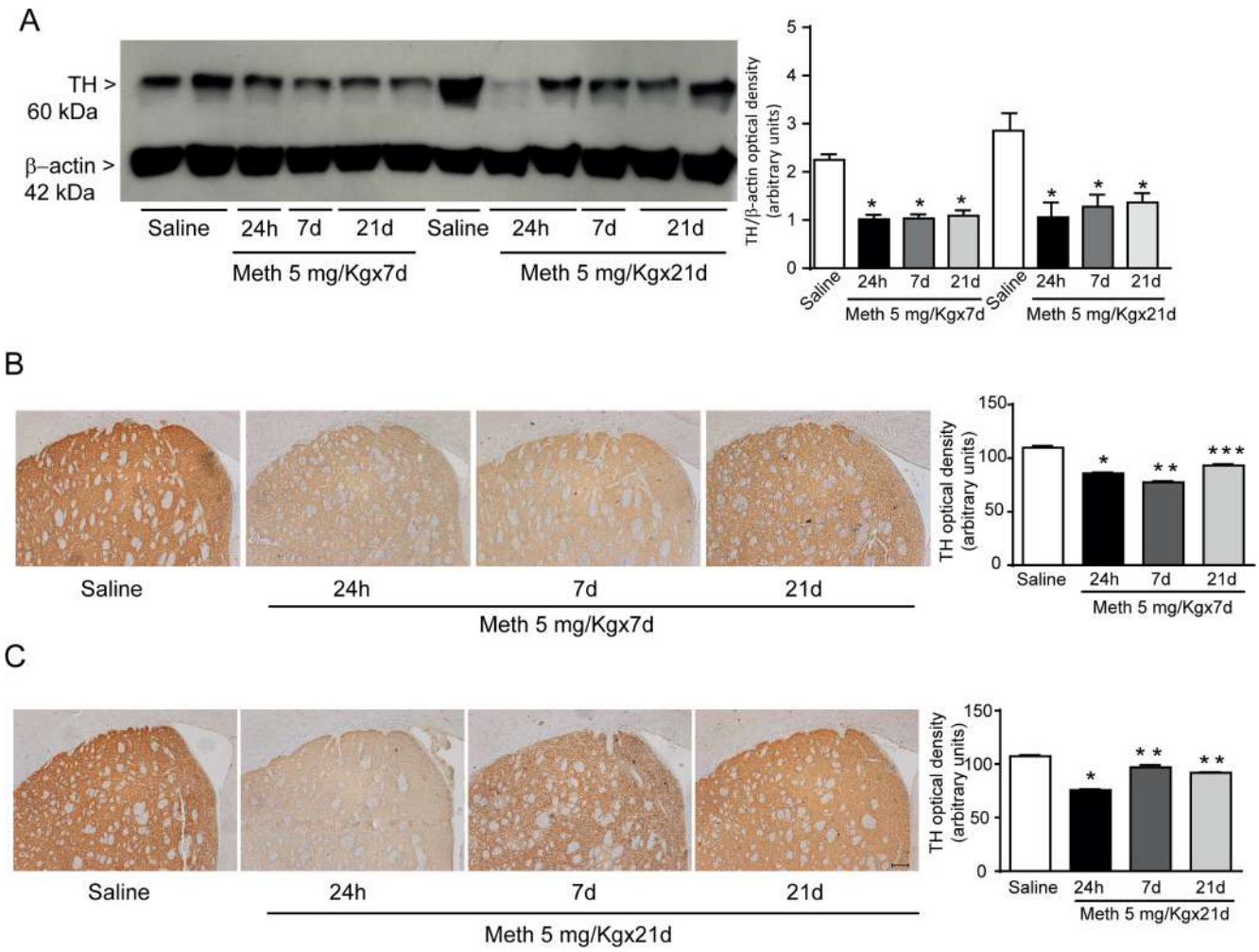

Fig. 3. Methamphetamine reduces tyrosine-hydroxylase immune-reactivity in the sub-acute and chronic time-course protocol. Immune-blot analysis demonstrates a significant reduction in TH protein levels in the dorsal striatum in both sub-acute and chronic administration protocols (5 mg/Kg × 7 d or 5 mg/Kg × 21 d) (shown in **A**) (*$p < 0.0001$ *vs.* saline). In panel **B**, immune-histochemistry shows a significant reduction of TH protein levels at 24 h and 7 d, and a partial recovery at 21 d after the last Meth administration according to the sub-acute time-course protocol (*$p < 0.0001$ *vs.* saline; **$p < 0.0001$ *vs.* saline and Meth 24 h; *** $p < 0.0001$ *vs.* saline, Meth 24 h and Meth 7 d). As shown in panel **C**, TH levels were significantly reduced at 24 h after the last Meth administration according to the chronic time-course protocol. At 7 d and 21 d of Meth withdrawal, there is a partial recovery of TH, which in any case, remains significantly lower than Controls (saline treated-mice; *$p < 0.0001$ *vs.* saline; **$p < 0.0001$ *vs.* saline and Meth 24 h). Scale bar 100 μm.

Meth administration lasting up to three weeks (chronic time-course protocol). This is evident both in representative pictures of Fig. 3C, left item, and from values expressed by the graph of Fig. 3C. Although the number of daily administration was prolonged up to 21 d, we failed to document a further decrease of TH levels at 7 d compared with 24 h (graph of Fig. 3C), which instead was present following a 7 d daily treatment (graph of Fig. 3B). In contrast, the recovery which we documented in the graph of Fig. 3B at 21 d of withdrawal was already present in the graph of Fig. 3C at 7 d of withdrawal. This apparent discrepancy is likely to rely on the time intervals between the first Meth injection and the sacrifice which was 28 d for the graph of Fig. 3B (when 21 d of withdrawal were considered) and, again 28 d, for the graph of Fig. 3C (when 7 d of withdrawal were considered). No additional recovery was observed in the graph of Fig. 3C when Meth withdrawal was protracted for a longer time interval (up to three-fold, 21 d, compared with 7d, Fig. 3C and Fig. 3B, respectively). Therefore, it seems that a 5 mg/Kg daily administration of Meth produces a maximum of neurotoxicity in 14 days; after this time interval recovery takes place and this happens even when Meth is protracted for additional 14 days. In fact, TH staining following 21 d of daily Meth administration is comparable to TH staining measured at 14 d following Meth administration. After these time intervals, TH levels increase. This is consistent with the finding that TH levels at 14 d following the beginning of Meth (5 mg/Kg, daily) 7 d exposure were not decreased when adding further daily doses (up to 21). Similarly, TH levels at 28 d following the beginning of Meth were not surpassed at 42 d (adding further 14 d of recovery time). Thus, prolonging the withdrawal period three-fold (from 7 d to 21 d) does not add a significant recovery of striatal TH, which at any rate, remains significantly lower than Controls.

2.3. Neither acute nor chronic protocols of Meth administration alter significantly nigral neurons

None of the experimental protocols being tested so far produces a noticeable alteration in the number of nigral neurons as reported in the representative pictures of Fig. 4. In detail, as shown in Fig. 4A no evident decrease in TH-positive nigral cell bodies was detected at 1 h, 24 h, or 7 d following an acute protocol of Meth administration (5 mg/Kg × 5, 2 h apart in a single day). Similarly, no effect was detectable in Fig. 4B following a chronic protocol of Meth administration (daily doses of 5 mg/Kg × 21 d) neither at 1 d nor at 7 d or 21 d following the last Meth injection. As shown consistently by a number of studies, when the effects Meth produce a moderate decrease (roughly a half) of striatal DA

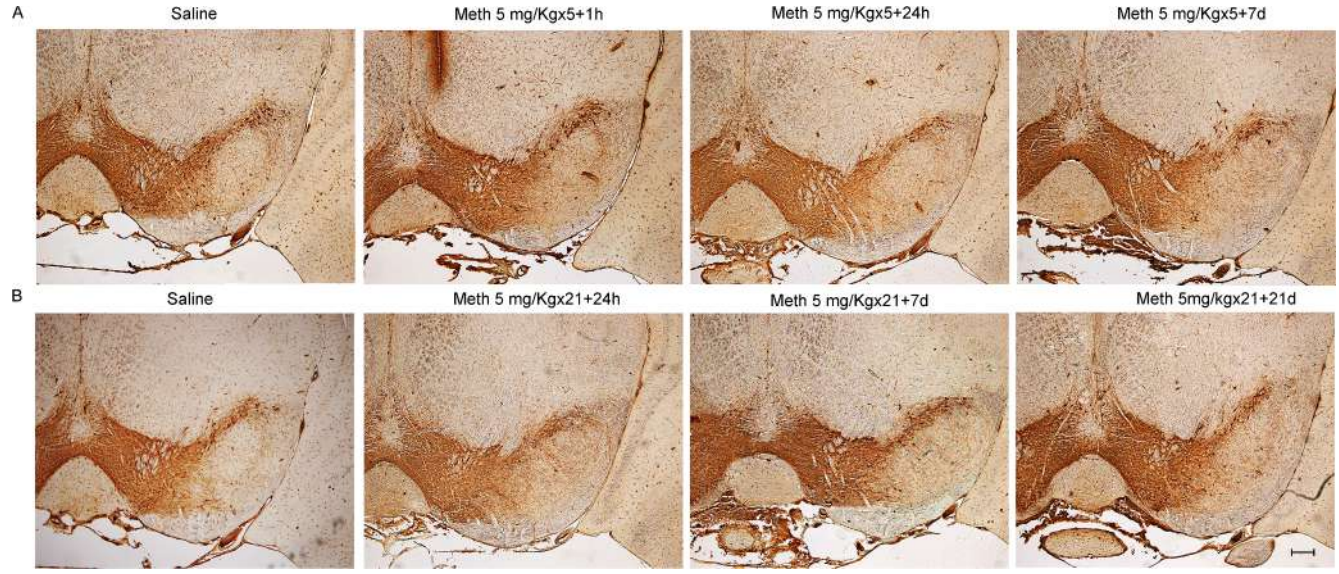

Fig. 4. Representative tyrosine-hydroxylase-immune-staining following acute and chronic methamphetamine administration in the *substantia nigra.* As shown in **A** no evident decrease in TH positive nigral cell bodies was detected at 1 h; 24 h; or 7d following an acute protocol of Meth administration (5 mg/Kg × 5, 2 h apart in a single day). Similarly, no effect was detectable in **B** following a chronic protocol of Meth administration (daily doses of 5 mg/Kg × 21 d) neither at 1 d nor at 7 d or 21 d following the last Meth injection. As shown consistently by a number of studies, when the effects Meth produce a moderate decrease (roughly a half) of striatal DA terminals detected either as TH immune-staining (or VMA2/DAT immune-staining/DA levels) no noticeable decrease in nigral neurons can be observed. This was described instead when a massive striatal depletion of DA terminals occurs (Sonsalla et al., 1996; Ares-Santos et al., 2014; Moratalla et al., 2017; Limanaqi et al., 2018). Scale bar 200 μm.

terminals detected either as TH immune-staining (or VMA2/DAT immune-staining/DA levels) no noticeable decrease in nigral neurons can be observed. This was described instead when a massive striatal depletion of DA terminals occurs (Sonsalla et al., 1996; Ares-Santos et al., 2014; Moratalla et al., 2017; Limanaqi et al., 2018).

2.4. Meth persistently increases striatal alpha-synuclein immune-staining in sub-acute and chronic time-course protocols only

In Fig. 5A, left item, representative pictures at different time intervals following acute Meth protocol (5 mg/Kg × 5, 2 h apart) are reported. In these pictures, Meth increases striatal α-syn immune-staining only transiently, at 1 h after administration, while these levels fall back below control values at 24 h and 7 d after a single day of multiple Meth injections. This is clearly expressed by numbers of the graph of Fig. 5A. These data clearly diverge from those obtained by measuring striatal TH. In fact, striatal TH was similar to Controls at 1 h, while α-syn was significantly lower than Controls at 24 h and 7 d following a multiple administration in a single day. On the other hand, α-syn increases significantly only transiently, at 1 h following multiple daily injections, while it decreases at 24 h and 7 d. In detail, at 7 d striatal α-syn was even lower than Controls suggesting that a loss of TH terminals might have reduced baseline striatal α-syn levels without providing for an increase in striatal α-syn synthesis. These data indicate a discrepancy between Meth-induced neurotoxicity and Meth-induced α-syn expression. The early and transient increase in striatal α-syn protein at 1 h occurred in the absence of any significant change of striatal TH protein. On the other hand, when a frank TH decrease was evident, at 24 h, and mostly 7 d following Meth, α-syn levels were similar or lower than controls. This markedly contrasts with a steady and significant increase in striatal α-syn which was detected following a multiple (both 7 d and 21 d) daily injection protocol, as shown in Fig. 5B and C. In fact, representative pictures of Fig. 5B and C provide an image of a steady increase in α-syn in the dorsal striatum at each time interval. Such an increase, which occurs already at 24 h, is not modified at 7 d and 21 d following a week of daily 5 mg/kg Meth injections. Thus, a steady increase of α-syn is observed at different time intervals following the sub-acute protocol. When a daily Meth administration was prolonged for three weeks (chronic protocol) the increase in α-syn was slightly different at 24 h and 7 d compared with 21 d of Meth withdrawal (42 d following the first Meth injection). Thus, Meth-induced increase of α-syn needs multiple days of Meth injections to occur steadily, while the amount depends on the number of daily injections. This was evident when comparing α-syn levels following seven Meth injections (Fig. 5B, left item and graph) with that induced by twenty-one injections (Fig. 5C, left item and graph). A remarkable difference was noticed between multiple injections in a single day compared with multiple days of single Meth injections. In the former case, only a transient (at 1 h) increase of α-syn could be detected, which vanished at 24 h and 7 d. Remarkably, Meth-induced loss in striatal TH immune-staining and Meth-induced increase in striatal α-syn immune-staining clearly diverge at specific time intervals. In fact, as reported in Fig. 3, the loss of nigro-striatal TH following Meth is persistent along each time interval (up to 21 d) and each protocol of protracted Meth administration. Nonetheless, it is worth of noting that following a sub-acute and chronic protocol of Meth administration (Fig. 3B and C) there is a significant recovery of striatal TH levels (at 21 d following the sub-acute treatment, and at both 7 d and 21 d following the chronic treatment) which does not occur for α-syn levels (Fig. 5B and C, respectively). In addition, following the chronic protocol, α-syn levels further increase at 21 d compared with 24 h and 7 d of Meth withdrawal. These data indicate that (i) Meth-induced increase of striatal α-syn does not depend on the severity of Meth-induced nigro-striatal toxicity; (ii) Meth-induced increase of striatal α-syn is not reverted during Meth withdrawal, when it may augment at longer time intervals. This latter point suggests a persistent switch in the rate of α-syn synthesis and/or clearance within the striatum. Altogether results indicate that all protocols produce neurotoxicity but only when Meth administration is reiterated for several days, α-syn levels are consistently increased for a long-time interval of Meth withdrawal. In contrast, Meth toxicity is mitigated over the withdrawal time. This discrepancy is not surprising considering the molecular mechanisms which are known to govern Meth-induced neurotoxicity in comparison with those events which are known to produce Meth-induced plasticity. Thus, the persistent increase in α-syn

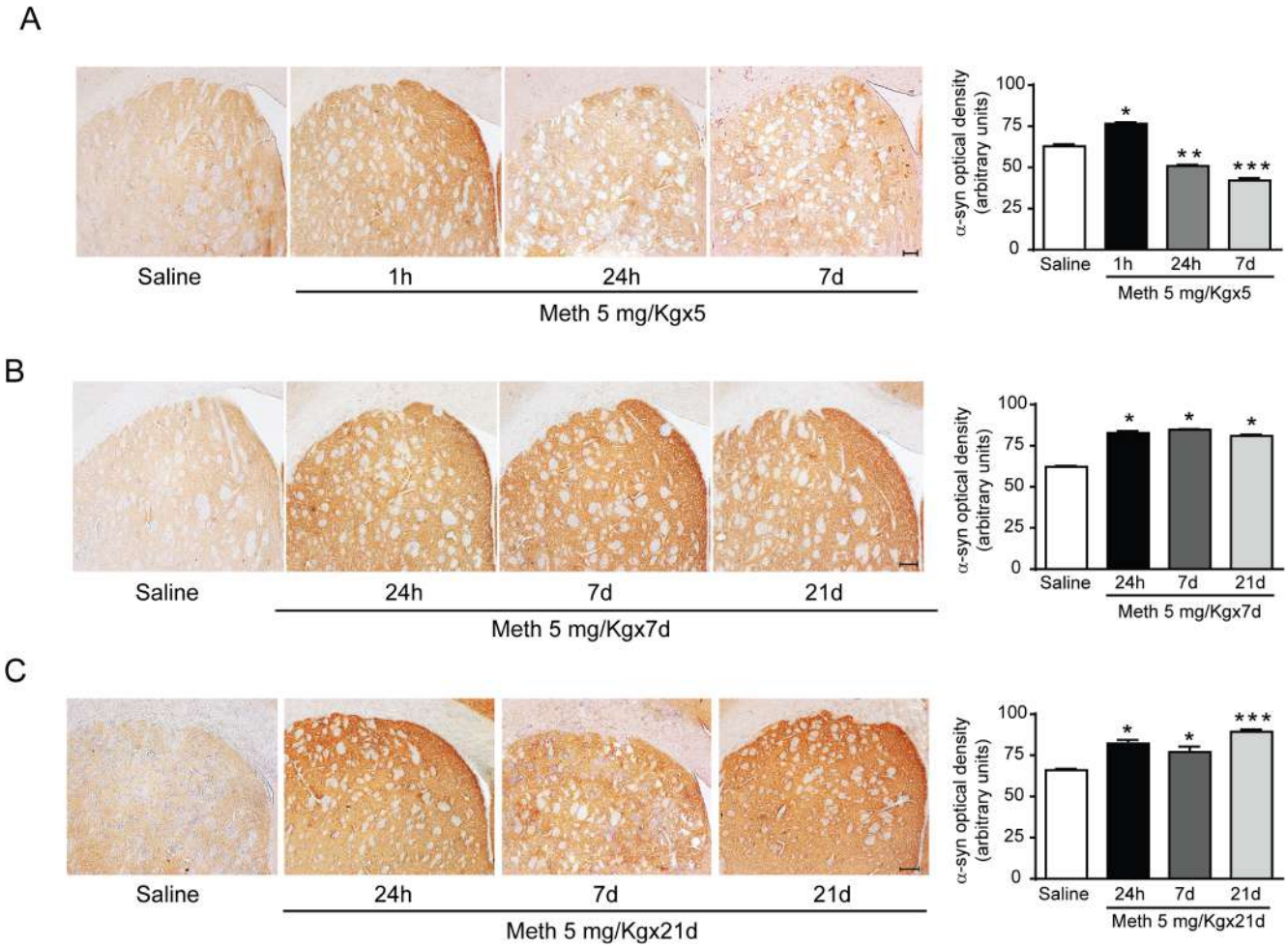

Fig. 5. Methamphetamine increases alpha-synuclein immune-reactivity in the acute, sub-acute and chronic time-course protocols. Immune-histochemical analysis shows a remarkable increase of α-syn protein in acute time-course protocol at 1 h after the last administration of Meth. This increase is no longer evident at 24 h and 7 d (panel **A**, $*p < 0.0001$ *vs.* saline; $**p < 0.0001$ *vs.* saline and Meth 1 h; $*** p < 0.0001$ *vs.* saline, Meth 1 h and Meth 24 h). When administered according to sub-acute and chronic time-course protocols, Meth significantly increases α-syn immune-reactivity at any time of withdrawal analyzed (5 mg/Kg × 7 and 5 mg/Kg × 21, panel **B** and **C**, respectively; in **B** $*p < 0.0001$ *vs.* saline; in **C** $*p < 0.0001$ *vs.* saline; $**p < 0.0001$ *vs.* saline and Meth 24 h; $*** p < 0.0001$ *vs.* saline, Meth 24 h and Meth 7 d). Scale bar 100 μm.

following Meth might be considered within a scenario of Meth-induced epigenetic-driven plasticity. It is well known that, although Meth toxicity and epigenetics greatly rely on DA release (Schmidt et al., 1985; Stone et al., 1988; Li et al., 2015; Biagioni et al., 2009), the threshold dose which is required to produce these events is different. In fact, Meth produces epigenetic effects even when it is administered at very low doses such as those used to induce behavioral sensitization, which do not necessarily produce toxicity, while toxic events require high cumulative Meth doses. Most importantly, sensitization strongly depends on daily Meth administration over repeated days while neurotoxicity is quickly obtained by multiple injections in a single day. This calls for considering the hypothesis that Meth-induced long-lasting α-syn over-expression may play a role in Meth-induced sensitization. This hypothesis would be worth to be explored in a behavioral context. In any case, Meth-induced persistent α-syn overexpression represents a plastic phenomenon, which called for assessing Meth-induced persistent changes in the regulation of *SNCA*.

2.5. Genomic analysis of SNCA

In search for potential mutations induced by Meth administration in *SNCA* following these experimental conditions, we carried out both a mutation analysis and Copy Number Variation (CNVs) of *SNCA* in 12 mice (N = 9, Meth- and N = 3, saline-treated mice) for the acute time-course protocol and 24 mice for the sub-acute (N = 9, Meth- and N = 3, saline-treated) and chronic (N = 9, Meth- and N = 3, saline-treated) time-course protocols. We could not identify any mutations or variations in the copy number of *SNCA* in any experimental groups (Fig. 6).

2.6. Identification of DNA regions containing CpG islands within the SNCA promoter

To date, information on CpG islands within *SNCA* promoter is available for *rattus norvegicus* genome (Jiang et al., 2014). To identify CpG islands within *SNCA* promoter in the mouse, online database and bioinformatics tools were applied. NCBI Gene (https://www.ncbi.nlm.nih.gov), identified a unique region containing CpG islands of the *SNCA* mouse promoter in Chromosome 6, spanning from 60,829,051 Mb to 60,829,238 Mb (reference genome: GRCm38/mm10). This 237 bp region contains 8 CpG islands, and BLAST multiple alignment (Basic Local Alignment Search Tool, https://blast.ncbi.nlm.nih.gov/Blast.cgi) revealed 88% homology with the DNA sequence of *rattus norvegicus* containing the CpG islands reported by Jiang et al. (2014). Considering these data, the 237 bp DNA region was selected for the methylation analysis (Fig. 7).

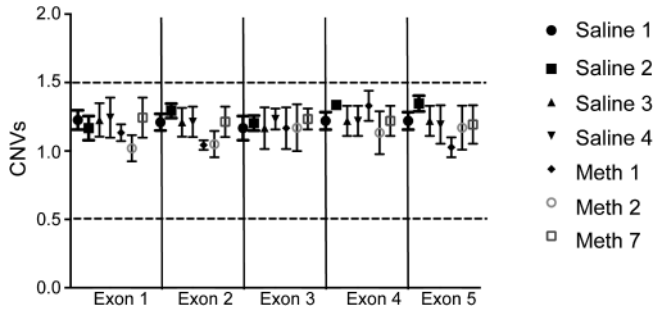

Fig. 6. Evaluation of gross deletions and duplications (CNVs) within *SNCA*. The plot shows the absence of deletions and duplications in mice treated with Meth 5 mg/Kg × 5, 2 h apart (METH1, METH2, METH7) sacrificed at 1 h, and four Controls (SAL1, SAL2, SAL3 and SAL4). The x-axis shows the genomic region analyzed, as reported in Table 2. The Y-axis shows the amount of DNA measured through qRT-PCR. Value of 1 corresponds to a diploid genomic region; values of 0.5 and 1.5 (evidenced by the dotted lines) are considered the cut-off values for heterozygous deletion or duplication, respectively. The minimum and maximum values for the standard deviation correspond to 0.8 and 1.2, respectively.

2.7. The increase in alpha-synuclein protein levels induced by Meth relates to Meth-induced demethylation in the SNCA promoter

*2.7.1. **Acute time-course protocol** (Fig. 8)*

The effects of Meth administration (5 mg/kg × 5, 2 h apart) on SDS-PAGE immune-blotting of striatal α-syn and demethylation of *SNCA* promoter were evaluated in a total of 12 mice (N = 9, Meth- and N = 3, saline-treated animals) sacrificed at 1 h, 24 h and 7d after the last Meth administration. Immune-blot analysis was very similar to previous data reported in Fig. 5A showing a consistent increase in α-syn protein levels at 1 h after the last Meth injection. However, such an increase did not persist at 24 h and 7 d following such an acute protocol. This is shown by representative immune-blots of Fig. 8A, and by densitometric analysis of all blots reported in the graph of Fig. 8A. The Methylated DNA Immune-precipitation (MeDIP) assay allows quantifying the DNA methylation level within selected DNA regions. The assay identified a marked percentage of hypomethylation within CpG islands of the mouse *SNCA* promoter. When DNA from Meth-treated mice was compared with Controls at 1 h following Meth, the percentage of demethylation was 92.66%, ranging from 76.6 up to 98.5 compared with Controls. In contrast, no differences in methylation levels were observed in Meth-treated mice at 24 h and 7d after Meth (Fig. 8B).

2.7.2. Both sub-acute and chronic time-course protocol produce a remarkable and persistent demethylation of CpG islands within SNCA promoter (Fig. 9)

The effects of a sub-acute and chronic protocol (Fig. 9A and B, respectively) of Meth administration were analyzed on immune-blots of striatal α-syn and MeDIP assay of striatal *SNCA* promoter (Fig. 9C and D). The results of the sub-acute protocol were obtained from a total of 12 mice (N = 9, Meth- and N = 3, saline-treated animals). The results of the chronic protocol of Meth administration were obtained from a total of 12 mice (N = 9, Meth- and N = 3, saline-treated animals). In both sub-acute (Fig. 9A) and chronic (Fig. 9B) time-course protocols Meth produces a steady increase in α-syn blots. Similarly, Meth produces a consistent and steady demethylation of *SNCA* promoter following both sub-acute (Fig. 9C) and chronic (Fig. 9D) time-course protocols. Remarkably, demethylation of *SNCA* promoter was still remarkable at 21 d following the last Meth administration independently of the cumulative dose of Meth (7 × 5 = 35 mg/Kg or 21 × 5 = 105 mg/Kg). This indicates the occurrence of a marked and persistent epigenetic alteration of *SNCA* following a wide range of Meth doses, which was already present after 1 week of daily Meth administration. The amount of demethylation within *SNCA* promoter was comparable between a week and three weeks of daily Meth treatment. In fact, in both protocols, the epigenetic effects reached almost the maximal intensity (roughly 90% of demethylation within CpG islands).

In detail, a sub-acute treatment of 7 d produces marked hypomethylation in mice sacrificed after 24 h (% hypomethylation ranging between 94% and 97.2%), 7 d (% hypomethylation ranging between 98.1% and 99%), and 21d (% hypomethylation ranging between 84.8% and 85.8%). Therefore, a Meth treatment of 7 d produces a steady percentage of hypomethylation at 24 h and 7 d (average percentage 96.23% and 98.43% respectively), which persists at 21 d (average percentage 85.1%, $*p < 0.0001$) (Fig. 9C).

Prolonging Meth treatment for 21d reproduces a marked

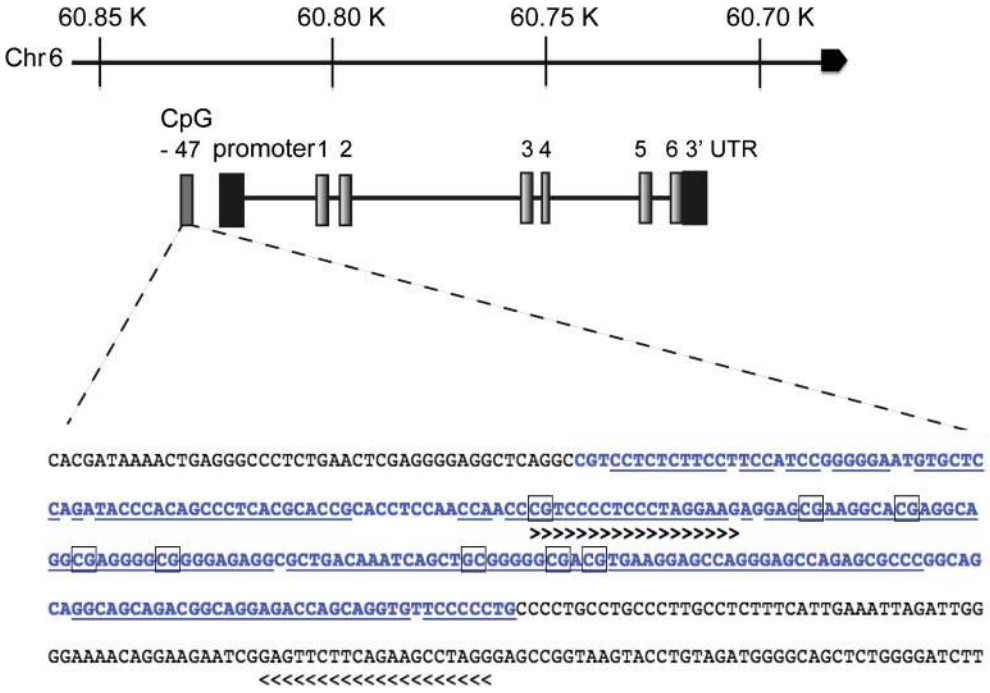

Fig. 7. DNA region containing CpG islands within *SNCA* promoter in the mouse. The figure shows the localization of the mouse *SNCA* on chromosome 6, and the insert shows the promoter region of 237 bp. *Rattus norvegicus* sequence is shown in blue (Jiang et al., 2014), mouse sequence in black. The underlined region is the homologous DNA region between *Rattus norvegicus* and mouse. This region contains 8 CpG islands shown in the black boxes. The arrows indicate the primers used for *SNCA* MeDIP analysis.

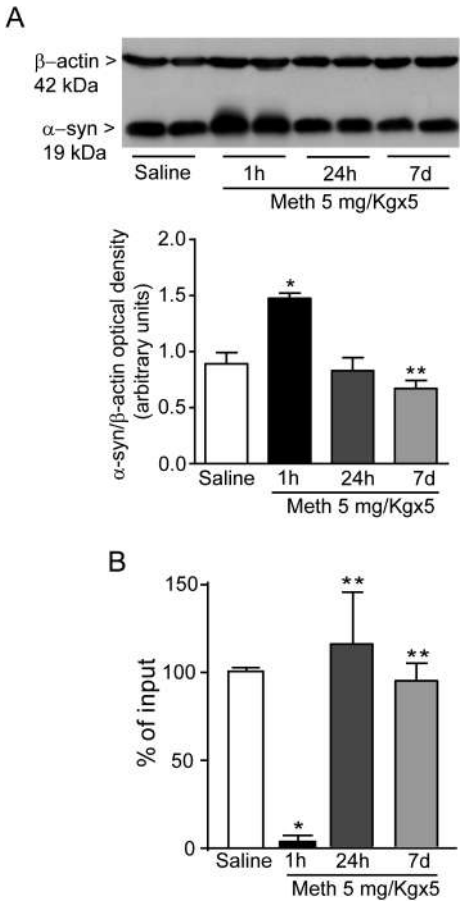

Fig. 8. Methamphetamine increases alpha-synuclein protein levels and promotes hypomethylation of *SNCA* promoter in the acute time-course protocol. In panel **A**, immune-blot analysis demonstrates a significant increase in α-syn protein levels at 1 h. Densitometric analysis was obtained as the mean ± S.E.M calculated from three blots. The figure shows a representative gel of the mean values quantified in the graph as arbitrary units (*$p < 0.0001$ *vs.* saline; **$p < 0.0001$ *vs.* saline and Meth 1 h). In panel **B**, hypomethylation of *SNCA* promoter following acute Meth administration (5 mg/Kg × 5, 2 h apart). In this experimental condition, significant *SNCA* hypomethylation was observed only at 1 h of Meth withdrawal, while no changes were observed at 24 h and 7 d (*$p = 0.0036$; **$p = 0.05$ *vs.* Meth 1 h).

hypomethylation in mice sacrificed after 24 h (% hypomethylation ranging between 90% and 94.1%), 7d (% hypomethylation ranging between 87.6% and 90.3%), and 21d (% hypomethylation ranging between 71% and 88%).

Similar to a 7 d Meth treatment, the 21 d chronic treatment produces a steady hypomethylation at 24 h and 7 d (average percentage 91.4% and 94% respectively), which persists significantly at 21 d (average percentage 82.1%) (Fig. 9D).

2.8. Alpha-synuclein immune-gold staining increases persistently only after reiterated daily Meth administration

The occurrence of an extensive demethylation within *SNCA* promoter, which steadily persisted at 3 weeks of Meth withdrawal, calls for a quantitative assessment of α-syn molecules within striatal cells following both acute (a single day of multiple Meth injections) and chronic (21 days of single injections) protocols of Meth administration.

2.8.1. A single day of multiple Meth injections transiently alters alpha-synuclein immune-gold particles within striatal neurons (Fig. 10)

Fig. 10 reports representative pictures from striatal cells stained with α-syn immune-gold particles (10 nm diameter, arrows) following a single day of multiple Meth administrations (5 mg/Kg × 5, 2 h apart). Saline-treated cell shows a few α-syn immune-gold particles. When administered according to the acute time-course protocol, Meth increases α-syn immune-gold particles both in the nucleus and cytosol at 1 h but not at 24 h or 7 d. In the graph of Fig. 10 the number of immune-gold particles is expressed as a percentage of control. At 1 h after the last Meth injection, a robust increase in α-syn immune-gold particles occurs, which vanishes at 24 h and 7 d after Meth administration.

2.8.2. Chronic Meth administration produces a dramatic and persistent increase in alpha-synuclein immune-gold particles (Fig. 11)

Representative micrographs from striatal cells stained for α-syn immune-gold particles (diameter = 10 nm, arrows). Only a few α-syn immune-gold particles are detected in a control cell. When administered according to a chronic protocol (5 mg/Kg × 21 d), Meth induces a remarkable increase in α-syn particles both in the nucleus and cytoplasm, which is present at 24 h following the last Meth injection and persists at 7 and even at 21 days of Meth withdrawal. In the graph of Fig. 11 the persistent increase is reported as a percentage of Controls (saline-treated mice). It is remarkable that the highest number of α-syn immune-gold particles were counted at the longest time interval of Meth withdrawal.

2.9. Chronic Meth administration produces a widespread increase in brain alpha-synuclein

As shown in Fig. 12A, upper line, representative hippocampal slices show a considerable α-syn immune-staining from a control mouse. This is robustly increased following a daily Meth administration for 7 d when observed at 21 d of Meth withdrawal. Remarkably, such an increase was enhanced at 21 d of Meth withdrawal when daily Meth administration was prolonged for 21 d. Similar findings were noticed for the piriform cortex and the ventral striatum, mostly the olfactory tubercle (Fig. 12B lower line). Other representative areas shown in Fig. 13A (isocortex); Fig. 13B (dorsal striatum); Fig. 13C (*substantia nigra*) confirm the widespread nature of the increase in α-syn immune-staining. This is the case of the sensorimotor iso-cortex (Fig. 13A) which extends just above the white matter and corpus callosum surrounding the dorsal striatum (Fig. 13B) and the *substantia nigra* (Fig. 13C). It is remarkable how the ventromedial aspect of the *substantia nigra pars compacta* which extends its dendrites in the *reticulata* is much more stained compared with the lateral part, which lends substance to different parts of the mosaic (more the striosomes) affected by Meth (Granado et al., 2010). This representative overview, which is consistent along different groups of mice, witnesses for the occurrence of a Meth-induced brain alteration characterized by a spread increase of *a*-syn, which is reminiscent of a degenerative synucleinopathy.

3. Discussion

In the present manuscript we provide evidence that Meth administration, when prolonged for a few weeks, persistently induces nigrostriatal DA denervation, where partial recovery reaches a plateau which remains significantly lower than Controls. When a chronic administration of Meth is carried out, an increase of striatal α-syn occurs, which persists up to three weeks following Meth withdrawal. Remarkably, striatal α-syn immune-staining is further increased during the late withdrawal period, which follows a chronic protocol of daily Meth administration. This phenomenon is neither associated with mutations in the *SNCA* gene sequence, nor with multiplication of *SNCA*. In contrast, we report a strong demethylation within a specific DNA region, which is expected to be the mouse *SNCA* promoter based on the homology with *SNCA* promoter sequence available for *rattus norvegicus* (Jiang et al., 2014). We identified this region based on database (https://www.ncbi.nlm.nih.gov), and bioinformatics tools which identified a unique region containing CpG islands of the *SNCA* mouse

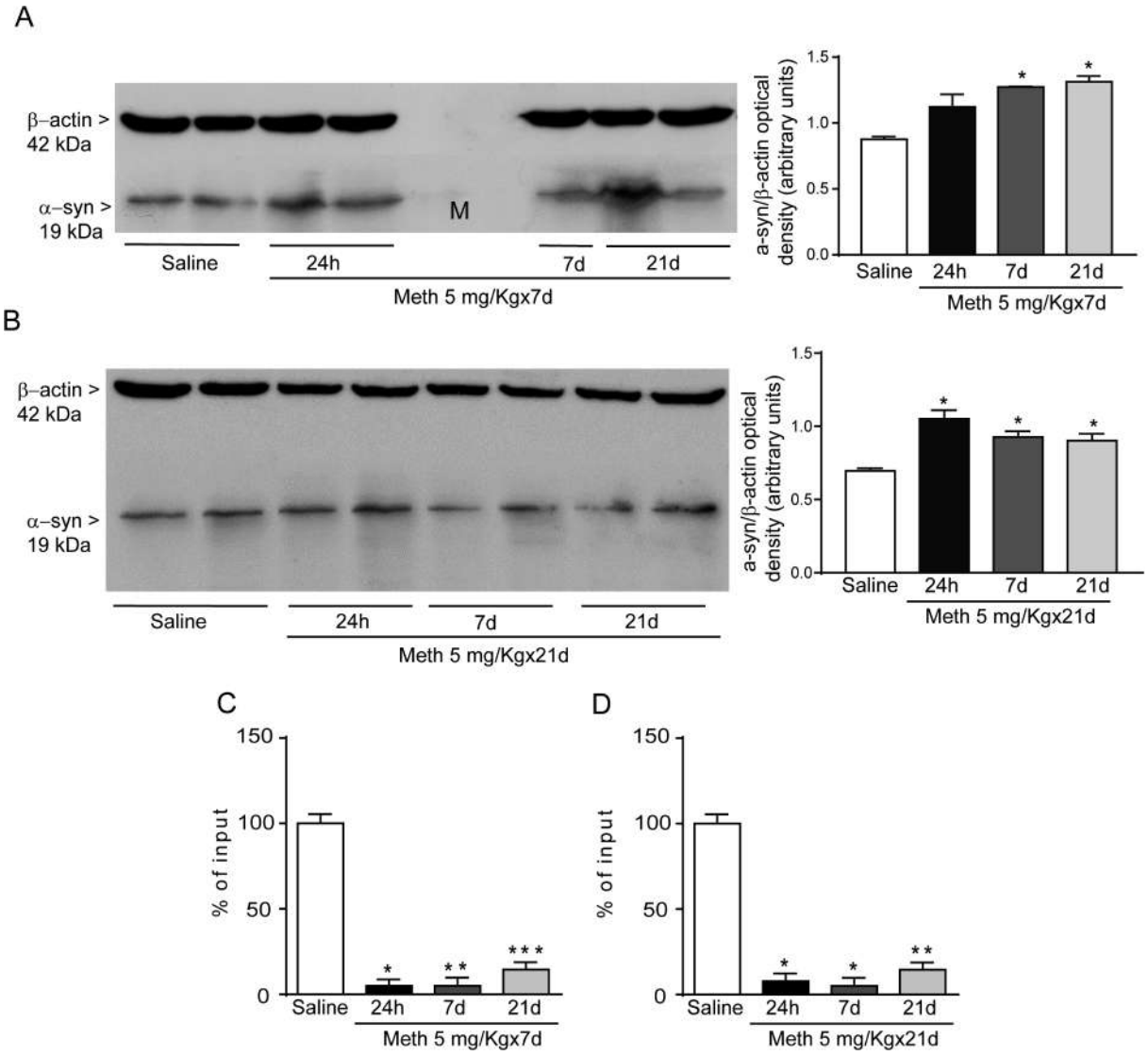

Fig. 9. Methamphetamine increases alpha-synuclein protein levels and promotes hypo-methylation of *SNCA* promoter in the sub-acute and chronic time-course protocols. In panel **A**, immune-blot analysis demonstrates a significant increase in α-syn protein levels at 7 d which persists at 21 d after the last administration of Meth according to the sub-acute (5 mg/Kg × 7 d) time-course protocol (*$p = 0.0016$ *vs.* saline alone). Similar results are obtained when Meth is administered according to the chronic (5 mg/Kg × 21 d) time-course protocol as shown in panel **B** (*$p = 0.0125$ *vs.* saline alone). Densitometric analysis was obtained as the mean ± S.E.M calculated from three blots. The figure shows two representative gels of the mean values plotted in the graphs of panel **A** and **B**. In panel **C** and **D,** a consistent hypomethylation of *SNCA* promoter following a sub-acute and chronic treatment is shown (5 mg/Kg × 7 d and 5 mg/Kg × 21 d, in **C** and **D**, respectively; in **C** *$p < 0.0001$ *vs.* saline alone; **$p < 0.0001$ *vs.* saline and Meth 24 h; ***$p < 0.0001$ *vs.* Meth 24 h and Meth 7 d; in **D** *$p < 0.0001$ *vs.* saline alone; **$p < 0.0001$ *vs.* saline and Meth 7 d).

promoter in Chromosome 6, spanning from 60,829,051 Mb to 60,829,238 Mb (reference genome: GRCm38/mm10). This region contains 8 CpG islands. When BLAST multiple alignment (https://blast.ncbi.nlm.nih.gov/Blast.cgi) was applied, this region revealed 88% homology with the DNA sequence of the *SNCA* promoter in *rattus norvegicus* reported by Jiang et al. (2014). The amount of demethylation of the *SNCA* promoter proceeded even at 21 d of Meth withdrawal. In line with this, the amount of α-syn immune-gold particles increased over time even when Meth administration was withdrawn. In fact, α-syn immune-gold particles reach the highest level at the longest time interval of Meth withdrawal tested so far (up to 21 d). It is important to notice that such a persistent and always increasing α-syn accumulation is independent of Meth toxicity (as measured by a loss of striatal TH immune-staining or a decrease in the blotted striatal TH protein). In fact, when striatal TH levels partially recover, the accumulation of striatal α-syn proceeds, continuing even beyond the time interval when TH levels reach a plateau. The occurrence of such a specific epigenetic alteration concomitant to and following chronic Meth administration appears as a plastic effect, which needs a reiterated drug administration to take place. In fact, following a classic protocol of Meth toxicity based on multiple Meth injections (5 mg/Kg, 2 h apart, in a single day), despite a significant striatal TH loss is documented at 24 h and 7 d, neither lasting changes in α-syn levels nor persistent demethylation in the *SNCA* promoter are detected. Altogether this evidence witnesses for an independency between Meth-induced nigro-striatal toxicity and Meth-induced α-syn overexpression, being the latter effect the consequence of a long-lasting and progressive epigenetic effect.

Increase of α-syn in the brain is commonly considered to be detrimental and it characterizes a number of neuropathological conditions which form a group of neurological disorders named synucleinopathies. For instance, the mutation in the gene coding for α-syn (*SNCA*) produces a genetic parkinsonism (PARK1), which is believed to derive from a gain of function of α-syn variants. A specific point mutation in the *SNCA* (p.G51D) instead, shifts the PD phenotype towards another

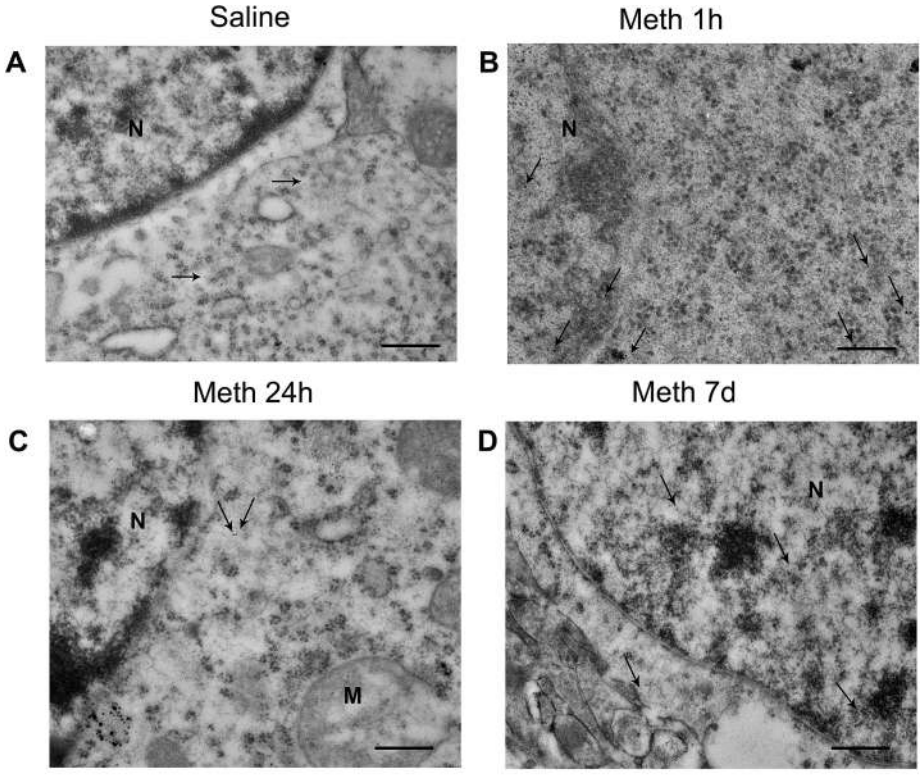

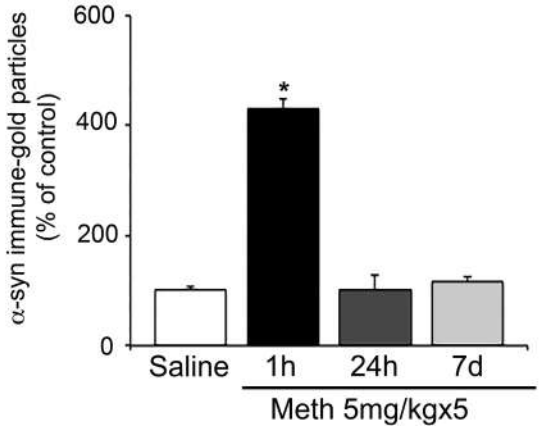

Fig. 10. Acute methamphetamine administration increases alpha-synuclein immune-gold particles at 1 h of withdrawal. Representative micrographs from striatal cells stained for α-syn immune-gold particles (10 nm in diameter) from saline- and Meth-treated mice at 1 h, 24 h, and 7 d of withdrawal. Panel **A** shows a representative cell from a Control (saline-treated) mouse which contains very few cytosolic α-syn immune-gold particles (arrows). At 1 h of withdrawal, acute Meth administration (5 mg/Kg × 5, 2 h apart) robustly increases α-syn particles both in the nucleus and cytoplasm (arrows), as shown in panel **B**. Instead, at 24 h and 7 d of Meth withdrawal, the amount of α-syn particles (arrows) falls back nearly to control levels (panel **C** and **D**, respectively). The graph reports the stoichiometric count of α-syn immune-gold particles in striatal cells from Meth-treated mice expressed as a percentage of values obtained from Controls (saline-treated mice). The data indicate that, when Meth is administered according to an acute time-course protocol, it significantly increases α-syn only at short-time intervals (1 h) of withdrawal (*$p < 0.05$ with respect to saline). N = nucleus; M = mitochondria Scale bars A, C, D = 400 nm; B = 200 nm.

synucleinopathy named multiple system atrophy (MSA, Fares et al., 2014; Fujioka et al., 2014; Kiely et al, 2015). The α-syn protein itself in its native physiological conformation appears to be strongly detrimental when it is expressed in excess due to *SNCA* multiplication (PARK4). In this latter case, the disease phenotype, which may vary, is often more severe compared with that observed in sporadic PD. This is not surprising, since as shown by Burrè et al. (2013, 2015) a wide amount of native α-syn detaches from membrane binding and tends to spontaneous misfolding. Thus, an excess of α-syn is expected to overwhelm cell aggregates. Despite *SNCA* mutations occur rarely in persons affected by PD, the presence of α-syn aggregates is a hallmark of almost all PD phenotypes. This suggests that α-syn is constantly recruited during the natural history of PD in spite of its sporadic or genetic transmission and independently of the specific trigger which initiates the disease process. These facts cast the hypothesis that, in the molecular chain of events leading to neurodegeneration a key and constant step consists in increasing α-syn levels or reducing its proper metabolism. As a proof of concept in 2005 we firstly tested such an hypothesis to check whether an environmental stimulus known to affect the cell biology of DA neurons may also converge in increasing α-syn levels within these cells. Thus, we administered Meth, which apart from being a psychostimulant drug of abuse is a powerful neurotoxin for DA neurons. In line with the hypothesis, TH-immune-positive neurons of the *substantia nigra pars compacta* developed intense α-syn immune-fluorescence at a short-time interval following an acute experimental protocol of Meth administration (Fornai et al., 2005a). These neurons possess high levels of α-syn as shown by immune-blotted tissue micropunched from *substantia nigra* from Meth-exposed mice compared with Controls (Fornai et al., 2005a). These findings followed up a previous paper where the occurrence of α-syn-ubiquitin and parkin-positive bodies in the *substantia nigra* of Meth-treated mice was demonstrated (Fornai et al., 2004). These previous studies led us to hypothesize that, within the Meth-exposed brain, molecular mechanisms bridging drug abuse and neurodegenerative disorders may take place (Iacovelli et al., 2006). Consistently, these findings were backed up by Purisai et al. (2005), who found that MPTP increases α-syn immune-staining in the

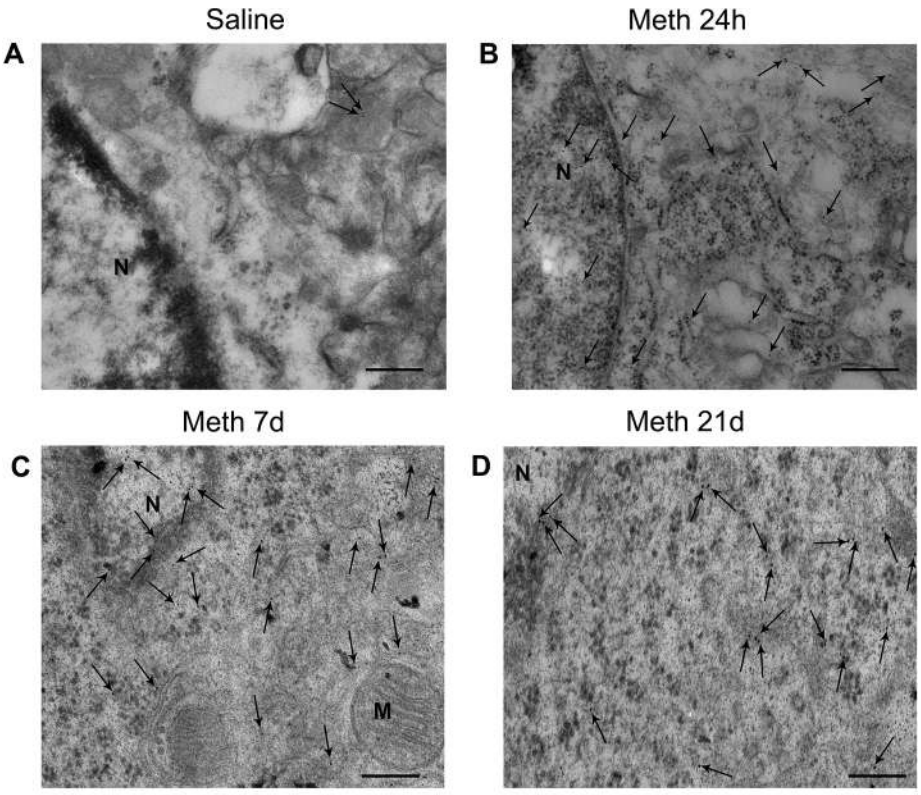

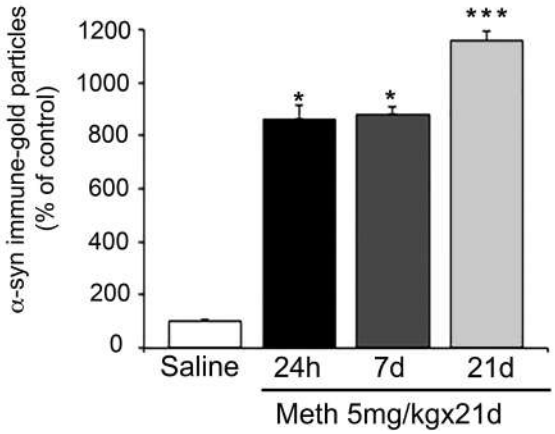

Fig. 11. Chronic methamphetamine administration produces a dramatic and persistent increase of alpha-synuclein immune-gold particles at each withdrawal time. Representative micrographs from striatal cells stained for α-syn immune-gold particles (10 nm in diameter) from saline- and Meth-treated mice at 24 h, 7 d, and 21 d of withdrawal. Panel **A** shows a representative cell from a saline-treated mouse which contains very few cytosolic α-syn immune-gold particles (arrows). When administered according to a chronic time-course protocol, Meth produces a robust increase in α-syn immune-gold particles both in the nucleus and cytoplasm (arrows) of striatal cells at 24 h of withdrawal (panel **B**), which persists at 7 d and 21 d of withdrawal (panel **C** and **D**, respectively). The graph provides a quantification of Meth-induced increase of α-syn immune-gold particles following a chronic protocol compared with Controls (saline-treated mice). (*$p < 0.05$ with respect to saline; **$p < 0.05$ with respect to Meth withdrawn at 24 h and 7 d). N = nucleus; M = mitochondria Scale bars A, B, C = 200 nm; D = 100 nm.

substantia nigra of primates, and McCormack et al. (2008) who demonstrated that, following MPTP α-syn accumulates as a proteinase K resistant misfolded protein. These data strengthened the hypothesis that environmental factors acting on protein synthesis or metabolism may lead to synucleinopathies by triggering α-syn accumulation and structural alterations. Thus, according to Vance et al. (2010) exposure to environmental neuro-toxicants may produce a higher susceptibility to neurodegeneration by triggering either up-regulation and/or pathological modifications of α-syn. When trying to dissect the molecular events leading to environmentally-induced α-syn accumulation, it was demonstrated that α-syn accumulation was DA-dependent. In fact, *in vivo*, in DA-depleted striata, Meth was no longer able to increase α-syn immune-staining but this was re-established by administering D1-like DA receptor agonists. *In vitro* evidence related such an effect to the recruitment of beta-arrestin which is considered to be key in DA-related striatal sensitization and is recruited indeed during Meth exposure (De Blasi et al., 2003; Beaulieu et al., 2005, 2008; Beaulieu and Caron, 2008; Fornai et al., 2008). It is likely that a link exists between Meth-induced DA release, DA toxicity and overexpression of α-syn. However, as hypothesized by Vance et al. (2010) at that time it was puzzling to decipher in which way environmental factors increase α-syn expression and alteration. The present study provides direct evidence showing how Meth administration may increase α-syn through a profound and persistent effect on the *SNCA* promoter region. Due to previous evidence which indicated a role of DA receptors in increasing α-syn protein following Meth administration, we analyzed the effects of Meth upon *SNCA* promoter in a brain area where DA storage is more abundant. This is why we investigated such an effect at striatal level. It is well known that Meth toxicity mostly involves striatal DA terminals while neuronal cell bodies in the *substantia nigra* and striatum may be affected as well (Wagner et al., 1980a, b; Schmidt et al., 1985; Sonsalla et al., 1996; Hirata and Cadet, 1997; Zhu et al., 2006; Granado et al., 2010, 2011a, 2011b; Ares-Santos et al., 2012, 2014; Moratalla et al., 2017). Striatal neurons remain a pivot for Meth-induced plasticity and

Fig. 12. Methamphetamine-induced increase in limbic (hippocampal, piriform and olfactory) alpha-synuclein-immune-staining. As shown in **A**, upper line, representative hippocampal slices show a considerable α-syn immune-staining from a control mouse. This is robustly increased following a daily Meth administration for 7 d when observed at 21 d of Meth withdrawal. Remarkably, such an increase was enhanced at 21 d of Meth withdrawal when daily Meth administration was prolonged for 21 d. Similar findings were noticed for the piriform cortex and the ventral striatum, mostly the olfactory tubercle (in **B**, lower lane). Scale bar 200 μm.

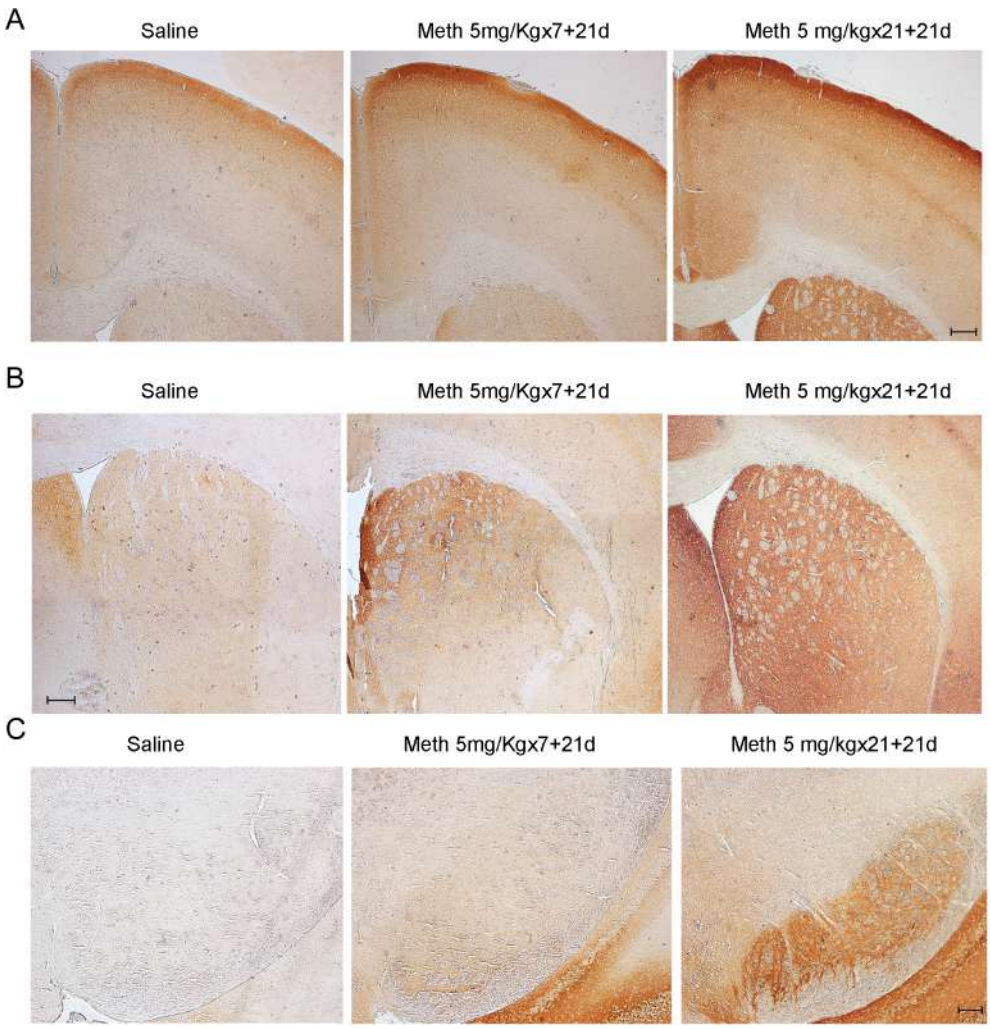

Fig. 13. Alpha-Synuclein-immune-staining of iso-cortex, dorsal striatum and *substantia nigra* following acute and chronic methamphetamine administration. Other representative areas confirm the widespread nature of Meth-induced α-syn immune-staining. This is the case of the sensorimotor iso-cortex (in **A**, upper lane) which extends just above the white matter and corpus callosum surrounding the dorsal striatum (in **B**, middle lane) and the *substantia nigra* (in **C**, lower lane). This representative overview is reminiscent of a degenerative synucleinopathy. Scale bar 200 μm.

epigenetic alterations and play an important role in long-lasting behavioral changes produced by Meth administration.

When tested on nigral neurons, Meth-induced overexpression of α-syn was associated only with two-fold demethylation of the *SNCA* promoter region compared with Controls. In detail, demethylation of the *SNCA* promoter never reached 50% in any CpG islands (Jiang et al., 2014). The data provided here at striatal level indicate that the amount of demethylation in the *SNCA* promoter region surpasses 95% (20-fold control values), and mostly, provide evidence for a persistent effect which remains steady at 21 days of Meth withdrawal. Such a strong effect may be due to several issues; the method used here, which consists in antibody-mediated detection of methylated cytosine and represents the most sensitive and specific tool to quantify the amount of DNA methylation. Another crucial point consists in the amount of striatal compared with nigral DA levels. Such a difference slightly varies for animal species and strains, although from a general standpoint this ranges between 10-fold and 15-fold for striatal compared with nigral DA levels. If one assumes that DA is a pivot in the expression of α-syn (Lazzeri et al., 2007) including the quote deriving from epigenetic stimulation, the different effect might be explained. Again, going back to the raw data shown here, it is intriguing to note the remarkable increase in α-syn protein which was detected by immune-gold stoichiometry compared with SDS-PAGE immune-blotting. It is likely that these methods grasp differently the protein amount. In fact, according to Vance, and mostly considering delayed times of withdrawal used here, it is plausible that a great part of α-syn is present as misfolded protein aggregates which do not run in gel electrophoresis as native α-syn. This may justify the great difference between immune-gold electron microscopy and immune-blotting. Similarly, this consideration may apply to the lower amount detected when α-syn is not measured in situ at ultrastructural level. Starting from our previous studies at nigral level, the present study moves the focus on the effects induced by Meth at striatal level disclosing novel avenues related to addiction and neurodegeneration. In fact, an increase of α-syn within striatal neurons is well established in Huntington's disease where α-syn deleteriously interacts with Huntingtin (Herrera and Outeiro, 2012; Poças et al., 2015) thus worsening the physiopathology of HD. In fact, a direct correlation was drawn between α-syn levels and the amount of neuropathology in HD (Corrochano et al., 2012a; Tomás-Zapico et al., 2012). Remarkably, as reported by Corrochano et al (2012b) α-syn levels modulate Huntington's disease in mice even considering disease phenotype and age at onset. Thus, the role of α-syn in the physiopathology of medium size striatal neurons is key since its deletion mitigates HD symptoms while its overexpression worsens the disease phenotype (Corrochano et al 2012b; Tomás-Zapico et al., 2012). Considering the data reported in the present manuscript and classic studies reviewed by Jakel and Maragos (2000) the role of DA in producing Meth toxicity seems to apply also to non-DA neurons since most of its epigenetic effects are grounded on DA release (Cadet et al., 2010b; Godino et al., 2015; Limanaqi et al., 2018). Finally, a role of α-syn in behavioral sensitization and addiction should be considered in the light of the present data. In fact, the remarkable increase in α-syn which we report representatively within hippocampus and other limbic regions such as the olfactory tubercle and the piriform cortex suggests that the increase in α-syn may contribute significantly to the process of behavioral sensitization. Again, some brain area where Meth produces a remarkable increase in α-syn is relatively poor of DA terminals, which lends substance to the hypothesis that DA *per se* is not sufficient to sustain the sensitization process induced by Meth, and other chemical species, such as oxidative endogenous compounds, are key for producing epigenetic alterations (Limanaqi et al., 2018).

In any case, apart from the strong take-home messages discussed above, the smoldering impression we seem to get from all these data is the ambiguous significance of α-syn overexpression in the brain. Intriguingly, a similar cautious approach was adopted very recently in an opinion article hypothesizing novel vistas on α-syn in the brain in health and disease (Espay et al., 2019). In this scenario, we have to consider the chance that, despite a discrepancy exists at chronic time intervals between TH and α-syn expression, this still might reflect a transient phenomenon. In fact, prolonged exposure (over several months) to high levels of α-syn may finally trigger neurodegeneration. This is also related to the natural trend of native α-syn to misfold, which is expected to be enhanced during prolonged time intervals. This hypothesis remains open and deserves dedicated investigations.

4. Experimental procedures

4.1. Animals

C57 black 6/J, 8 weeks-old male mice (Charles River Calco, Mi, Italy, N = 120) were housed in small cages (N = 6 per cage; cage length = 27 cm; cage width = 21 cm; cage height = 14 cm). They were kept under controlled environmental conditions (temperature = 22 °C; humidity = 40%) with food and water ad libitum and with a 12 h light/dark cycle. All these measures were kept constant all over the study since the effects of Meth markedly vary depending on housing conditions beyond temperature, such as cage size and number of animals per cage (Fornai et al., 2004). Mice were handled in accordance with the Guidelines for Animal Care and Use of the National Institutes of Health, and adequate measures were taken to minimize animal pain and discomfort. The experimental protocol was approved by the local Ethical Committee, and by the Ministry of Health. As a mouse strain, we chose C57/6J-Black mice based on previous literature and our previous studies in different mouse strains. In fact, the inbred C57-Black mice possess a very stable DA phenotype and are mostly sensitive to DA neurotoxins. This allows increasing the statistical power to detect even small differences in each biological value under analysis. Again, amongst various C57-Black strains, we preferred the 6/J compared with 6/N where a spontaneous *SNCA* variant was reported (Schlüter et al., 2003). As a species, mice were preferred over rats due to a high sensitivity to Meth which, amongst rodents, makes them closer to primates. In addition, C57 Black mice when administered Meth doses which are toxicant for the DA system, are more resistant to 5-HT toxicity which is more evident in rats (O'Dell et al., 2012). Such an additional target of Meth toxicity might confound the significance of the present study, which is centered on DA-related disorders, DA-projecting areas and α-syn as a detrimental protein related to DA pathways, including post-synaptic target neurons.

4.2. Methamphetamine administration and experimental design

A total of 120 mice were dedicated to these experiments. A group of 48 mice was dedicated to electron microscopy, while 72 mice were sacrificed for immune-histochemistry, protein assay, and DNA analysis. These latter 72 mice were divided into different experimental groups (N = 24 each) according to three experimental protocols.

These protocols consisted in different dosing and timing of Meth or saline administration. Methamphetamine (Meth, Sigma Aldrich Saint Louis, MO, U.S.A., Authorization n° SP/096, 05.15.2016, granted by the Italian Ministry of Health, was dissolved in saline and it was injected i.p. in a volume of 200 μL; saline was administered i.p. at the same volume). In the first subgroup (N = 24) mice were sacrificed at different time intervals (1 h, N = 6; 24 h, N = 6; 7 d N = 6) following the last Meth injection; an additional group of mice (N = 6) was administered saline (Controls). Meth was administered at the dose of 5 mg/Kg (×5, 2 h apart). From now on we refer to this protocol as acute time-course protocol since Meth was administered in a single day with a short-time interval between starting Meth and sacrifice.

In the second subgroup of mice (N = 24) Meth (5 mg/Kg), was injected daily, for 7 d. These mice were sacrificed at different time intervals (24 h, N = 6; 7 d, N = 6; 21 d, N = 6) after the last administration; an additional group (N = 6) was administered saline (Controls). From now on we refer to this protocol as sub-acute time-course protocol

(5 × 7) since Meth was administered for 7 d.

The third subgroup of mice (N = 24) received Meth (at the dose of 5 mg/Kg) daily, for 21 d and they were sacrificed at different time intervals (24 h, N = 6; 7 d, N = 6; 21 d, N = 6) after the last injection; an additional group (N = 6) was administered saline (Controls). This protocol was named chronic time-course protocol (5 × 21). This corresponds to the most chronic condition since Meth treatment lasted 21 d. In both sub-acute and chronic protocols, the longest withdrawal between the last Meth injection and sacrifice was 21 d, which allows detecting the persistence of the effects induced by Meth. One should consider that, while in the sub-acute protocol the longest time interval between the first Meth injection and sacrifice was 28 d, in the chronic protocol the longest time interval was protracted up to 42 d. Again, the cumulative dose of Meth in the sub-acute time-course protocol was 35 mg/Kg (7 × 5 mg/Kg), whilst this dose rose up to 105 mg/Kg (21 × 5 mg/Kg) in the chronic time-course protocol. These mice were sacrificed by deep chloral hydrate anesthesia and their brains were quickly removed and processed according to different procedures.

Since the critical data were obtained following acute and chronic protocols, further experiments were aimed at analyzing ultrastructural morphometry according to both acute and chronic time-course protocols. For these additional experiments we used 48 mice, which were sacrificed according to the acute (N = 24) or the chronic (N = 24) time-course protocol. In detail, according to the chronic protocol mice received Meth (at the dose of 5 mg/kg), once daily, for 21 d and they were sacrificed at different time intervals (24 h, N = 6; 7 d, N = 6; and 21 d, N = 6) after the last injection; an additional group (N = 6) was administered saline (Controls). Twenty-four mice were used in the acute protocol where they were administered Meth (N = 18, 5 mg/Kg × 5, 2 h apart), and they were sacrificed at 1 h (N = 6), 24 h (N = 6), and 7d (N = 6) after treatment; Control mice (N = 6) were administered saline. Each mouse from each protocol used for electron microscopy was perfused with a solution containing 2% paraformaldehyde and 0.1% glutaraldehyde under deep chloral hydrate anesthesia.

During and after each treatment mice were housed N = 6 per cage and they were kept under controlled environmental conditions (temperature = 22 °C; humidity = 40%) with food and water ad libitum with a 12 h light/dark cycle until sacrifice.

4.3. Post-sacrifice brain processing

In the first experimental block (N = 72), after sacrifice, the brains were quickly removed from the skull and they were divided into two hemispheres; one hemisphere was constantly used for immune-histochemical studies, while the other hemisphere was used either for immune-blot analysis, or DNA extraction for *SNCA* mutation detection, and methylation detection assay within *SNCA* promoter. In the second experimental block (N = 48) mice were perfused trans-cardially under deep chloral hydrate anesthesia. The brains were dissected and immersed at 4 °C, overnight, in the perfusing solution. Tissue blocks from striata at the same level of that used for other assays were post-fixed.

4.4. Immune-histochemistry

Since Meth administration may lead to nigro-striatal DA denervation, we carried out in all mice immune-histochemistry and Sodium Dodecyl Sulphate-PolyAcrylamide Gel Electrophoresis (SDS-PAGE) immune-blotting for Tyrosine-Hydroxylase (TH) to assess indirectly the loss of striatal DA innervation following different protocols of Meth administration, at different time intervals after the last Meth injection. In the same hemisphere, at the same striatal level, we analyzed the effects of Meth administration on TH and α-syn immune-histochemistry, while in the contralateral hemisphere either striatal TH and α-syn SDS-PAGE immune-blotting, or DNA analysis were carried out. For TH and α-syn immune-histochemistry the hemisphere was removed and placed in a fixing solution overnight. Mice specimens were fixed in Carnoy's solution (ethanol 60%, chloroform 30% and glacial acetic acid 10%), they were embedded in paraffin, and 10 μm thick tissue sections were cut and mounted on slides for immune-histochemical analysis, where TH and α-syn immune-reactivity were counted in serial sections to keep constant and comparable the level of analysis for both antigens. In detail, TH and α-syn immune-reactivity were carried out in the dorsal striatum at a level ranging between +0.62 mm and +0.74 mm from bregma according to the atlas of Franklin and Paxinos (1997). At this level, densitometric count was carried out. At the very same level we report the representative pictures for the sensorimotor iso-cortex, the ventral striatum including the olfactory tubercle, and the piriform cortex. Hippocampal staining for α-syn was reported for a rostrocaudal level ranging from −1.82 mm to −2.06 mm from bregma. When both immune-staining were carried out at nigral level, a range from −3.16 mm to −3.08 mm from bregma was scanned.

Tissue sections were de-waxed and antigen retrieval was carried out by exposing the slices to citrate buffer, pH 6.0, for 10 min. Brain slices were then incubated with 0.01% Triton X-100 (Sigma Aldrich, Milan, Italy) for 15 min and were soaked in 3% hydrogen peroxide to block endogenous peroxidase activity. Then, they were incubated overnight at 4 °C with mouse monoclonal anti-TH antibody (1:100; Sigma Aldrich; Antibody registry: AB_477560), rabbit anti- α-syn (1:100; Sigma Aldrich; Antibody registry: AB_10746104); the sections were incubated with anti-mouse or anti-rabbit biotinylated secondary antibodies (1:200; Vector Laboratories, Burlingame, CA, U.S.A.) for 1 h, at 22 °C. Peroxidase activity was revealed by using a solution containing 0.04% of 3,3′-diaminobenzidine-tetrahydrochloride (DAB; Sigma Aldrich) pH 7.6, for 3 min at 22 °C. The stained sections were dehydrated, cleared and coverslipped with Micromount (Diapath, Martinengo, BG, Italy). The specificity and quality of anti- α-syn immune-staining which was detected in brain slices was compared by using antibodies (1:100; Sigma Aldrich; Antibody registry: AB_10746104) and (1:300; BD; Antibody registry: AB_398108).

This was carried out in pilot staining in the present work and considering our previous studies as well as additional references where striatal α-syn immune-staining was carried out (Schlüter et al., 2003; Fornai et al., 2005a,b; Betarbet et al., 2006): for western blotting monoclonal anti-α-syn synuclein-1 (Transduction Labs, Betarbet et al., 2006). Data provided a signal which was similar to total α-syn (AB_52168; 1:200 in BSA 1% PBST; Abcam, Cambridge, UK), used by Novello et al. (2018) or human anti-α-syn (AB_36615, 1:1000, Abcam, UK) as used by Mulcahy et al. (2012). The data obtained with Sigma Aldrich were quite similar to the one we obtained with anti-α-Syn (Transduction Laboratories, Lexington, KY, USA) (Schlüter et al., 2003). The pilot studies for striatal α-syn immune-staining compared Sigma Aldrich antibodies with a presently available BD anti-α-syn antibody (AB_398108); both stainings were compared with classic striatal TH immune-staining in Fig. 1, which shows a higher specificity for Sigma compared with BD anti-α-syn- antibody. This staining was also comparable with that obtained using the α90 antibody both for immune-histochemistry and immune-cytochemistry (Totterdell et al., 2004).

4.4.1. Densitometric analysis of striatal alpha-synuclein and tyrosine-hydroxylase immune-staining

Intensity of striatal TH and α-syn immune-reactivity was semi-quantified by measuring relative optical densities. In fact, images were acquired at low magnification (2.5×) and antigen densitometry was calculated as the ratio between optical density in the dorsal striatum and that in the white matter (i.e. corpus callosum). Despite being a semi-quantitative assay, values were consistent with a very low S.E.M.

4.5. Immune-blotting

The hemisphere was placed on a wet paper placed on ice-cold Petri dish to dissect the rostral part of the dorsal striatum. Briefly, the lateral wall of the third ventricle was pulled aside, the anterior commissure

was removed and the rostral part of the dorsal striatum was dissected out and placed in an Eppendorf tube containing 250 µL of ice-cold lysis with phosphatase and protease inhibitor to be homogenized. An aliquot of the homogenate was used for protein assay. Proteins (30 µg) were separated on SDS-polyacrylamide gels (10%) and transferred on Immuno-PVDF membranes (Biorad, Milan, Italy) for 1 h. Membranes were blocked for 2 h in Tween-20 Tris-buffered saline (TTBS) (100 mM Tris-HCl, 0.9% NaCl, 1% Tween 20, pH 7.4) containing 5% non-fat dry milk. Membranes were incubated overnight at 4 °C with primary antibodies rabbit anti- α-syn (1:1000; Sigma Aldrich), or mouse anti-TH (1:5000; Millipore, Burlington, MA, U.S.A.). Membranes were washed 3 times with TTBS buffer and incubated for 1 h with secondary peroxidase-bound antibodies (anti-rabbit/anti-mouse, 1:3000; Calbiochem, Milan, Italy). Membranes incubated with mouse anti-TH antibody were stripped with a solution of distilled water and 3.5% acetic acid in the presence of 1% NaCl 5 M. Membranes were kept in this solution for 20 min, and then washed in TTBS (8 washes, 5 min each). This procedure was carried out since we used mouse antibodies against both TH and β-actin (mouse, 1:10,000; Sigma Aldrich). β-Actin was used as an internal standard for semi-quantitative protein measurement, so-called "house-keeping protein". Membranes were washed 3 times with TTBS buffer and then incubated for 1 h with secondary peroxidase-coupled antibody (anti-mouse, 1:3000; Calbiochem). Immune-staining was revealed by enhanced chemo-luminescence (GE Healthcare, Milan, Italy). Blots of TH and α-syn were assessed for optical density being normalized for β-actin blots (Software, ImageJ) and expressed as the mean ± S.E.M. calculated from three blots.

4.6. DNA extraction

The mouse striatal DNA following each experimental protocol (Meth- and saline-treated mice) was extracted by NucleoSpin® Tissue (Macherey Nagel GmbH & Co.KG, Dueren, Germany) according to the manufacturer's instructions.

4.7. Mutation analysis

The entire *SNCA* coding sequence (NM_001042451), as well as exon/intron boundaries and flanking intronic regions were analyzed by PCR and direct sequencing. The PCR assay was performed in 25 µL containing 50 ng genomic DNA, 2 mM $MgCl_2$, 25 µM primers, and 1U Taq polymerase (GoTaq® Flexi DNA Polymerase, Promega, Sunnyvale, CA, U.S.A.). PCR mix was amplified using the following cycle: 94 °C for 45 s, 58 °C for 30 s, 72 °C for 45 s (35 cycles), followed by a 6 min extension at 72 °C. PCR products were sequenced using ABI BigDye Terminator Sequencing Kit v.3.3 (Applied Biosystems, Foster City, CA, U.S.A.) and ABI 310 Genetic Analyzer (Applied Biosystems). Primer pair sequences are available in Table 1.

4.8. Quantitative PCR (qPCR)

qPCR was performed in a CFX Connect™ Real Time System (Bio-Rad Life Science, Hercules, CA, U.S.A.) using SYBR Green PCR Master (Applied Biosystems). The reaction was carried out with the same primers used for the sequence reaction (Table 1). The relative copy number was calculated through a ΔΔCT method, using ß-Globin as an internal reference. qPCR was carried out in triplicate for each sample. Ten µL SYBR Green PCR Master (Applied Biosystems), 0.5 µM of each primer and 5 ng of genomic DNA were used as amplification reagents acting in a 15 µL volume. The PCR reaction took place at 95 °C for 10 min, 95 °C for 30 s, 58 °C for 1 min (40 cycles).

4.9. Methylated DNA Immune-precipitation (MeDIP)

The samples were homogenized in a lysis buffer and genomic DNA was sonicated using the S220 AFA Ultrasonicator (Covaris Inc., Woburn, MA, U.S.A.). The sonicated DNA was immune-precipitated with a monoclonal antibody against 5-hydroxymethylcytosine (5-hmC) (Diagenode, Liège, Belgium) and it was incubated for 4 h at 4 °C. The DNA-antibody complex was enriched with Dynabeads Protein G (Life Technologies, Carlsbad, CA, U.S.A.) and it was digested with Proteinase K (Mohn et al., 2009). Both DNA fragments in the input and pulled-down fractions were purified with phenol-chloroform extraction followed by acid ethanol precipitation. Real-Time PCR was carried out to amplify a region corresponding to CpG Island identified within *SNCA* promoter. Real-Time PCR was amplified in a CFX Connect™ Real Time System (Bio-Rad Life Science) at 95 °C for 10 min, 95 °C for 2 min, 54 °C for 1 min (40 cycles) using the following primers: *SNCA,* FW = 5′-TCCCTAGGCTTCTGAAGAAC-3′ and RW = 5′-CGTCCCCTCCCTAGG AAG-3′; *GAPDH* (as an hypomethylated control) and *THS2B* primers (as an hypermethylated control) (Diagenode) were used as an internal reference. Percentage of methylation for CpG obtained was expressed by averaging the value of all CpGs per assay (0% non-methylated, 100% fully methylated). 5hmC MeDIP Real-Time PCR data were first normalized using the efficacy of each qPCR assay. The ratio IP/input was transformed in percentage.

4.10. Immune-gold-transmission electron microscopy

Tissue blocks from striata at the same level of that considered for immune-staining and SDS-PAGE immune-blotting were dissected for transmission electron microscopy (TEM). From these blocks, 50 µm thick sections were cut with a Vibratome following a coronal plane. All sections were obtained from blocks previously fixed in a solution containing 2.0% paraformaldehyde and 0.1% glutaraldehyde in 0.1 M PBS (pH = 7.4) for 90 min at 4 °C. This aldehyde concentration minimally covers antigen epitopes, while fairly preserving tissue trim (Fornai

Table 1
PCR primers of *SNCA*.

Exon	Primers
1	FW- GGGAAGGCATACTGATTTTT RW- AGCTGTGATGCACACGAA
2	FW- CACTTTAGTGATTTCTGAGTG RW- GTAGACAATGGCTCTTACAC
3	FW- TCCTGTTACCTATGATATATGT RW- GGTTATTGTGTGCATGACATTT
4	FW- CGTGCAGCACCTTGAAGA RW- GATCTGATAGTGGCAGGG
5	FW- TCTGTCACTTCACTGACAA RW- AACTGAGCACTTGTACGC

The table reports the primers used for analyzing the whole sequence of *SNCA* and detecting potential copy number variations. This was carried out in order to investigate whether various METH protocols may produce *SNCA* mutations already described in genetic PD or potential novel variants in *SNCA* which may affect the integrity of the nigro-striatal DA system.

Table 2
Genomic regions analyzed within *SNCA*.

nt	Gene- Exon	Chr.band	Genomic coordinates
338	*SNCA*-Exon 1	06qB3	60,827,793; 60,827,455
298	*SNCA*-Exon 2	06qB3	60,818,553; 60,818,255
419	*SNCA*-Exon 3	06qB3	60,815,971; 60,815,555
264	*SNCA*-Exon 4	06qB3	60,733,319; 60,733,055
154	*SNCA*-Exon 5	06qB3	60,732,209; 60,732,055

The table shows the genomic regions of *SNCA* which were analyzed to establish the presence/absence of mutations and gross deletions/duplications (copy number variations [CNVs]). In detail, the table reports the size of each *SNCA* region (nt = nucleotide), the exon (from 1 to 5), the chromosomal localization (Chr.band) and the genomic coordinates (GRCm38/mm10).

et al., 2005b). After removing the fixing solution, striatal sections were post-fixed in 1% OsO_4 for 1 h at 4 °C; they were dehydrated in ethanol and finally embedded in epoxy resin.

For ultrastructural morphometry, grids containing non-serial ultrathin sections (40–50 nm thick) were examined at TEM, at a magnification of 8000×.

Grids were analyzed in order to count immune-gold particles within 10 striatal neurons from each mouse from N = 6 mice per group (4 groups in the acute time-course protocol, and 4 groups in the chronic time-course protocol). Cells to be counted were carefully selected based on ultrastructural criteria, which were previously described for medium-sized striatal neurons (Fornai et al., 2001a,b; Lazzeri et al., 2007; Fornai et al., 2002).

Plain TEM was implemented by post-embedding immune-cytochemistry for antibodies against α-syn. At the end of the plain TEM or immune-cytochemistry, ultrathin sections were stained with uranyl acetate and lead citrate, and they were finally examined using a JEOL JEM-100SX TEM (JEOL, Tokyo, Japan).

4.10.1. Post-embedding immune-cytochemistry

Fixing and post-fixing solutions and the use of epoxy resin were validated in our previous studies for immune-gold-based ultrastructural morphometry (Fornai et al., 2001a,b, 2003; Lenzi et al., 2016). In fact, a combination of aldehydes, OsO_4, and epoxy resin allows a minimal epitope covering, while preserving sub-cellular architecture (Bendayan and Zollinger, 1983; D'Alessandro et al., 2004; Lenzi et al., 2016). In particular, OsO_4 binds to cell membranes, thus enhancing the contrast of cytosolic compartments while preventing membrane artifacts. Moreover, epoxy resin better preserves cell morphology compared with acrylic resin. Post-embedding procedure was carried out on ultrathin sections collected on nickel grids, which were incubated on droplets of aqueous sodium metaperiodate ($NaIO_4$), for 30 min, at 22 °C to remove OsO_4. Being an oxidizing agent, NaIO4 allows a closer contact between antibodies and antigens by removing OsO_4 (Bendayan and Zollinger, 1983). This step improves visualization of immune-gold particles specifically placed within a sharp context of cell integrity, and it allows the stoichiometric counting of immune-gold-stained proteins within each specific cell compartment. Then, grids were washed in PBS and they were incubated in a blocking solution containing 10% goat serum and 0.2% saponin for 20 min, at 22 °C. Grids were then further incubated with a primary antibody solution containing rabbit anti- α-syn (1:20; Sigma Aldrich), with 0.2% saponin and 1% goat serum in a humidified chamber overnight, at 4 °C. After washing in PBS, grids were incubated with the secondary antibody conjugated with gold particles (10 nm mean diameter for gold particle anti-rabbit, 1:30; BB International) diluted in PBS containing 0.2% saponin and 1% goat serum for 1 h, at 22 °C. Control sections were incubated with secondary antibody only. After washing in PBS, grids were incubated on droplets of 1% glutaraldehyde for 3 min; additional washing of grids on droplets of distilled water was carried out to remove salt traces and prevent uranyl acetate precipitation. Counts of immune-gold particles (10 nm) were performed directly at TEM at a magnification of 8000× (Lucocq et al., 2004) since this represents the minimal magnification at which immune-gold particles and all cell organelles can be concomitantly identified. We started to count immune-gold particles in striatal neurons from a grid square corner in order to scan the whole section within that grid square, which was randomly identified. Briefly, we counted the total number of immune-gold particles for α-syn placed either in the cytoplasm and within the nucleus of each cell. The mean of 10 cells from each striatum was considered, and the values from each group were expressed as the mean ± S.E.M. In order to match the data from ultrastructural morphometry with demethylation within *SNCA* promoter, we plotted the number of immune-gold particles in Meth-treated mice as a percentage of Controls (saline-treated mice).

4.11. Statistical analysis

All data are shown as the mean ± S.E.M. in each group. When the data were normalized to percentage values, data are reported as the percentage of the mean ± percentage of the standard error of the mean. Data were compared by using one-way ANOVA followed by *Bonferroni post-hoc* test for immune-histochemistry, immune-gold, SDS-PAGE immune-blotting and MeDIP analysis. Null Hypothesis H_0 was rejected when $P < 0.05$.

5. Funding sources

This research was funded by MINISTERO DELLA SALUTE (RICERCA CORRENTE 2019).

Declaration of Competing Interest

The authors declare no conflict of interests

Appendix A. Supplementary data

Supplementary data to this article can be found online at https://doi.org/10.1016/j.brainres.2019.05.035.

References

Ares-Santos, S., Granado, N., Oliva, I., O'Shea, E., Martin, E.D., Colado, M.I., Moratalla, R., 2012. Dopamine D(1) receptor deletion strongly reduces neurotoxic effects of methamphetamine. Neurobiol. Dis. 45, 810–820. https://doi.org/10.1016/j.nbd.2011.11.005.

Ares-Santos, S., Granado, N., Espadas, I., Martinez-Murillo, R., Moratalla, R., 2014. Methamphetamine causes degeneration of dopamine cell bodies and terminals of the nigrostriatal pathway evidenced by silver staining. Neuropsychopharmacology 39, 1066–1080. https://doi.org/10.1038/npp.2013.307.

Aubert, I., Guigoni, C., Håkansson, K., Li, Q., Dovero, S., Barthe, N., Bioulac, B.H., Gross, C.E., Fisone, G., Bloch, B., Bezard, E., 2005. Increased D1 dopamine receptor signaling in levodopa-induced dyskinesia. Ann. Neurol. 57, 17–26. https://doi.org/10.1002/ana.20296.

Baba, M., Nakajo, S., Tu, P.H., Tomita, T., Nakaya, K., Lee, V.M., Trojanowski, J.Q., Iwatsubo, T., 1998. Aggregation of alpha-synuclein in Lewy bodies of sporadic Parkinson's disease and dementia with Lewy bodies. Am. J. Pathol. 152, 879–884.

Barroso-Chinea, P., Thiolat, M.L., Bido, S., Martinez, A., Doudnikoff, E., Baufreton, J., Bourdenx, M., Bloch, B., Bezard, E., Martin-Negrier, M.L., 2015. D1 dopamine receptor stimulation impairs striatal proteasome activity in Parkinsonism through 26S proteasome disassembly. Neurobiol. Dis. 78, 77–87. https://doi.org/10.1016/j.nbd.2015.02.024.

Beaulieu, J.M., Caron, M.G., 2008. Looking at lithium: molecular moods and complex behaviour. Mol. Interv. 8, 230–241. https://doi.org/10.1124/mi.8.5.8.

Beaulieu, J.M., Sotnikova, T.D., Marion, S., Lefkowitz, R.J., Gainetdinov, R.R., Caron, M.G., 2005. An Akt/beta-arrestin 2/PP2A signaling complex mediates dopaminergic neurotransmission and behavior. Cell 122, 261–273. https://doi.org/10.1016/j.cell.2005.05.012.

Beaulieu, J.M., Marion, S., Rodriguiz, R.M., Medvedev, I.O., Sotnikova, T.D., Ghisi, V., Wetsel, W.C., Lefkowitz, R.J., Gainetdinov, R.R., Caron, M.G., 2008. A beta-arrestin 2 signaling complex mediates lithium action on behavior. Cell 132, 125–136. https://doi.org/10.1016/j.cell.2007.11.041.

Bendayan, M., Zollinger, M., 1983. Ultrastructural localization of antigenic sites on osmium-fixed tissues applying the protein A-gold technique. J. Histochem. Cytochem. 31, 101–109. https://doi.org/10.1177/31.1.6187796.

Berthet, A., Porras, G., Doudnikoff, E., Stark, H., Cador, M., Bezard, E., Bloch, B., 2009. Pharmacological analysis demonstrates dramatic alteration of D1 dopamine receptor neuronal distribution in the rat analog of L-DOPA-induced dyskinesia. J. Neurosci. 29, 4829–4835. https://doi.org/10.1523/JNEUROSCI.5884-08.2009.

Berthet, A., Bezard, E., Porras, G., Fasano, S., Barroso-Chinea, P., Dehay, B., Martinez, A., Thiolat, M.L., Nosten-Bertrand, M., Giros, B., Baufreton, J., Li, Q., Bloch, B., Martin-Negrier, M.L., 2012. L-DOPA impairs proteasome activity in parkinsonism through D1 dopamine receptor. J. Neurosci. 32, 681–691. https://doi.org/10.1523/JNEUROSCI.1541-11.2012.

Betarbet, R., Canet-Aviles, R.M., Sherer, T.B., Mastroberardino, P.G., McLendon, C., Kim, J.H., Lund, S., Na, H.M., Taylor, G., Bence, N.F., Kopito, R., Seo, B.B., Yagi, T., Yagi, A., Klinefelter, G., Cookson, M.R., Greenamyre, J.T., 2006. Intersecting pathways to neurodegeneration in Parkinson's disease: effects of the pesticide rotenone on DJ-1, alpha-synuclein, and the ubiquitin-proteasome system. Neurobiol. Dis. 22, 404–420. https://doi.org/10.1016/j.nbd.2005.12.003.

Biagioni, F., Pellegrini, A., Ruggieri, S., Murri, L., Paparelli, A., Fornai, F., 2009. Behavioural sensitisation during dopamine replacement therapy in Parkinson's disease is reminiscent of the addicted brain. Curr. Top Med. Chem. 9, 894–902. https://doi.org/10.2174/156802609789378245.

Burré, J., Vivona, S., Diao, J., Sharma, M., Brunger, A.T., Südhof, T.C., 2013. Properties of native brain α-synuclein. Nature 498, E4–E7. https://doi.org/10.1038/nature12125.
Burré, J., Sharma, M., Südhof, T.C., 2015. Definition of a molecular pathway mediating α-synuclein neurotoxicity. J. Neurosci. 35, 5221–5532. https://doi.org/10.1523/JNEUROSCI.4650-14.2015.
Cadet, J.L., Brannock, C., Krasnova, I.N., Ladenheim, B., McCoy, M.T., Chou, J., Lehrmann, E., Wood, W.H., Becker, K.G., Wang, Y., 2010. Methamphetamine-induced dopamine-independent alterations in striatal gene expression in the 6-hydroxydopamine hemiparkinsonian rats. PLoS One 5, e15643. https://doi.org/10.1371/journal.pone.0015643.
Cadet, J.L., Jayanthi, S., McCoy, M.T., Beauvais, G., Cai, N.S., 2010b. Dopamine D1 receptors, regulation of gene expression in the brain, and neurodegeneration. CNS Neurol. Disord. Drug Targets 9, 526–538 PMID: 20632973. PMCID: PMC3803153.
Cadet, J.L., Jayanthi, S., McCoy, M.T., Ladenheim, B., Saint-Preux, F., Lehrmann, E., De, S., Becker, K.G., Brannock, C., 2013. Genome-wide profiling identifies a subset of methamphetamine (METH)-induced genes associated with METH-induced increased H4K5Ac binding in the rat striatum. BMC Genomics 14, 545. https://doi.org/10.1186/1471-2164-14-545.
Callaghan, R.C., Cunningham, J.K., Sykes, J., Kish, S.J., 2012. Increased risk of Parkinson's disease in individuals hospitalized with conditions related to the use of methamphetamine or other amphetamine-type drugs. Drug Alcohol Depend. 120, 35–40. https://doi.org/10.1016/j.drugalcdep.2011.06.013.
Campbell, B.C., Li, Q.X., Culvenor, J.G., Jäkälä, P., Cappai, R., Beyreuther, K., Masters, C.L., McLean, C.A., 2000. Accumulation of insoluble alpha-synuclein in dementia with Lewy bodies. Neurobiol. Dis. 7, 192–200. https://doi.org/10.1006/nbdi.2000.0286.
Corrochano, S., Renna, M., Tomas-Zapico, C., Brown, S.D., Lucas, J.J., Rubinsztein, D.C., Acevedo-Arozena, A., 2012a. α-Synuclein levels affect autophagosome numbers in vivo and modulate Huntington disease pathology. Autophagy 8, 431–432. https://doi.org/10.4161/auto.19259.
Corrochano, S., Renna, M., Carter, S., Chrobot, N., Kent, R., Stewart, M., Cooper, J., Brown, S.D., Rubinsztein, D.C., Acevedo-Arozena, A., 2012b. α-Synuclein levels modulate Huntington's disease in mice. Hum. Mol. Genet. 21, 485–494. https://doi.org/10.1093/hmg/ddr477.
D'Alessandro, D., Mattii, L., Moscato, S., Bernardini, N., Segnani, C., Dolfi, A., Bianchi, F., 2004. Immunohistochemical demonstration of the small GTPase RhoA-A on epoxy-resin embedded sections. Micron 35, 287–296. https://doi.org/10.1016/j.micron.2003.10.001.
De Blasi, A., Capobianco, L., Iacovelli, L., Lenzi, P., Ferrucci, M., Lazzeri, G., Fornai, F., Picascia, A., 2003. Presence of beta-arrestin in cellular inclusions in metamphetamine-treated PC12 cells. Neurol. Sci. 24, 164–165. https://doi.org/10.1007/s10072-003-0111-5.
Desplats, P., Lee, H.J., Bae, E.J., Patrick, C., Rockenstein, E., Crews, L., Spencer, B., Masliah, E., Lee, S.J., 2009. Inclusion formation and neuronal cell death through neuron-to-neuron transmission of alpha-synuclein. Proc. Natl. Acad. Sci. U.S.A. 106, 13010–13015. https://doi.org/10.1073/pnas.0903691106.
Doherty, K.M., Silveira-Moriyama, L., Parkkinen, L., Healy, D.G., Farrell, M., Mencacci, N.E., Ahmed, Z., Brett, F.M., Hardy, J., Quinn, N., Counihan, T.J., Lynch, T., Fox, Z.V., Revesz, T., Lees, A.J., Holton, J.L., 2013. Parkin disease: a clinicopathologic entity? JAMA Neurol. 70, 571–579. https://doi.org/10.1001/jamaneurol.2013.172.
Espay, A.J., Vizcarra, J.A., Marsili, L., Lang, A.E., Simon, D.K., Merola, A., JosephKA, Fasano A., Morgante, F., Savica, R., Greenamyre, J.T., Cambi, F., Yamasaki, T.R., Tanner, C.M., Gan-Or, Z., Litvan, I., Mata, I.F., Zabetian, C.P., Brundin, P., Fernandez, H.H., Standaert, D.G., Kauffman, M.A., Schwarzschild, M.A., Sardi, S.P., Sherer, T., Perry, G., Leverenz, J.B., 2019. Revisiting protein aggregation as pathogenic in sporadic Parkinson and Alzheimer diseases. Neurology 92 (7), 329–337. https://doi.org/10.1212/WNL.0000000000000692.
Fares, M.B., Ait-Bouziad, N., Dikiy, I., Mbefo, M.K., Jovičić, A., Kiely, A., Holton, J.L., Lee, S.J., Gitler, A.D., Eliezer, D., Lashuel, H.A., 2014. The novel Parkinson's disease linked mutation G51D attenuates in vitro aggregation and membrane binding of α-synuclein, and enhances its secretion and nuclear localization in cells. Hum. Mol. Genet. 23, 4491–4509. https://doi.org/10.1093/hmg/ddu165.
Farrer, M., Kachergus, J., Forno, L., Lincoln, S., Wang, D.S., Hulihan, M., Maraganore, D., Gwinn-Hardy, K., Wszolek, Z., Dickson, D., Langston, J.W., 2004. Comparison of kindreds with parkinsonism and alpha-synuclein genomic multiplications. Ann. Neurol. 55, 174–179. https://doi.org/10.1002/ana.10846.
Ferese, R., Modugno, N., Campopiano, R., Santilli, M., Zampatti, S., Giardina, E., Nardone, A., Postorivo, D., Fornai, F., Novelli, G., Romoli, E., Ruggieri, S., Gambardella, S., 2015. Four copies of SNCA responsible for autosomal dominant Parkinson's disease in Two Italian Siblings. Parkinsons Dis. 2015, 546462. https://doi.org/10.1155/2015/546462.
Fornai, F., Gesi, M., Saviozzi, M., Lenzi, P., Piaggi, S., Ferrucci, M., Casini, A., 2001a. Immunohistochemical evidence and ultrastructural compartmentalization of a new antioxidant enzyme in the rat substantia nigra. J. Neurocytol. 30, 97–105.
Fornai, F., Piaggi, S., Gesi, M., Saviozzi, M., Lenzi, P., Paparelli, A., Casini, A.F., 2001b. Sub-cellular localization of a glutathione-dependent dehydroascorbate-reductase within specific rat brain regions. Neuroscience 104, 15–31.
Fornai, F., Gesi, M., Lenzi, P., Ferrucci, M., Pellegrini, A., Ruggieri, S., Casini, A., Paparelli, A., 2002. Striatal postsynaptic ultrastructural alterations following methylenedioxymethamphetamine administration. Ann. N.Y. Acad. Sci. 965, 381–398.
Fornai, F., Lenzi, P., Gesi, M., Ferrucci, M., Lazzeri, G., Busceti, C.L., Ruffoli, R., Soldani, P., Ruggieri, S., Alessandri, M.G., Paparelli, A., 2003. Fine structure and biochemical mechanisms underlying nigrostriatal inclusions and cell death after proteasome inhibition. J. Neurosci. 23, 8955–8966.
Fornai, F., Lenzi, P., Gesi, M., Soldani, P., Ferrucci, M., Lazzeri, G., Capobianco, L., Battaglia, G., De Blasi, A., Nicoletti, F., Paparelli, A., 2004. Methamphetamine produces neuronal inclusions in the nigrostriatal system and in PC12 cells. J. Neurochem. 88, 114–123.
Fornai, F., Lenzi, P., Ferrucci, M., Lazzeri, G., di Poggio, A.B., Natale, G., Busceti, C.L., Biagioni, F., Giusiani, M., Ruggieri, S., Paparelli, A., 2005a. Occurrence of neuronal inclusions combined with increased nigral expression of alpha-synuclein within dopaminergic neurons following treatment with amphetamine derivatives in mice. Brain Res. Bull. 65, 405–413. https://doi.org/10.1016/j.brainresbull.2005.02.022.
Fornai, F., Schlüter, O.M., Lenzi, P., Gesi, M., Ruffoli, R., Ferrucci, M., Lazzeri, G., Busceti, C.L., Pontarelli, F., Battaglia, G., Pellegrini, A., Nicoletti, F., Ruggieri, S., Paparelli, A., Südhof, T.C., 2005b. Parkinson-like syndrome induced by continuous MPTP infusion: convergent roles of the ubiquitin-proteasome system and alpha-synuclein. Proc. Natl. Acad. Sci. U.S.A. 102, 3413–3418. https://doi.org/10.1073/pnas.0409713102.
Fornai, F., Lenzi, P., Capobianco, L., Iacovelli, L., Scarselli, P., Lazzeri, G., De Blasi, A., 2008. Involvement of dopamine receptors and beta-arrestin in metamphetamine-induced inclusions formation in PC12 cells. J. Neurochem. 105, 1939–1947. https://doi.org/10.1111/j.1471-4159.2008.05284.x.
Fornai, F., Biagioni, F., Fulceri, F., Murri, L., Ruggieri, S., Paparelli, A., 2009. Intermittent Dopaminergic stimulation causes behavioral sensitization in the addicted brain and parkinsonism. Int. Rev. Neurobiol. 88, 371–398. https://doi.org/10.1016/S0074-7742(09)88013-6.
Frenzilli, G., Scarcelli, V., Fornai, F., Paparelli, A., Nigro, M., 2006. The comet assay as a method of assessment of neurotoxicity: usefulness for drugs of abuse. Ann. N.Y. Acad. Sci. 1074, 478–481. https://doi.org/10.1196/annals.1369.048.
Frenzilli, G., Ferrucci, M., Giorgi, F.S., Blandini, F., Nigro, M., Ruggieri, S., Murri, L., Paparelli, A., Fornai, F., 2007. DNA fragmentation and oxidative stress in the hippocampal formation: a bridge between 3,4-methylenedioxymethamphetamine (ecstasy) intake and long-lasting behavioral alterations. Behav. Pharmacol. 18, 471–481. https://doi.org/10.1097/FBP.0b013e3282d518aa.
Fujioka, S., Ogaki, K., Tacik, P.M., Uitti, R.J., Ross, O.A., Wszolek, Z.K., 2014. Update on novel familial forms of Parkinson's disease and multiple system atrophy. Parkinsonism Relat. Disord. 20, S29–S34. https://doi.org/10.1016/S1353-8020(13)70010-5.
Galvin, J.E., Uryu, K., Lee, V.M., Trojanowski, J.Q., 1999. Axon pathology in Parkinson's disease and Lewy body dementia hippocampus contains alpha-, beta-, and gamma-synuclein. Proc. Natl. Acad. Sci. U.S.A. 96, 13450–13455. https://doi.org/10.1073/pnas.96.23.13450.
Gasser, T., 1998. Genetics of Parkinson's disease. Ann. Neurol. 44, S53–S57. https://doi.org/10.1034/j.1399-0004.1998.5440401.x.
Gasser, T., 2007. Update on the genetics of Parkinson's disease. Mov. Disord. 22, S343–S350. https://doi.org/10.1002/mds.21676.
Godino, A., Jayanthi, S., Cadet, J.L., 2015. Epigenetic landscape of amphetamine and methamphetamine addiction in rodents. Epigenetics 10, 574–580. https://doi.org/10.1080/15592294.2015.1055441. Review.
Goedert, M., Clavaguera, F., Tolnay, M., 2010. The propagation of prion-like protein inclusions in neurodegenerative diseases. Trends Neurosci. 33, 317–325. https://doi.org/10.1016/j.tins.2010.04.003.
Granado, N., Ares-Santos, S., O'Shea, E., Vicario-Abejón, C., Colado, M.I., Moratalla, R., 2010. Selective vulnerability in striosomes and in the nigrostriatal dopaminergic pathway after methamphetamine administration: early loss of TH in striosomes after methamphetamine. Neurotox. Res. 18, 48–58. https://doi.org/10.1007/s12640-009-9106-1.
Granado, N., Ares-Santos, S., Oliva, I., O'Shea, E., Martin, E.D., Colado, M.I., Moratalla, R., 2011a. Dopamine D2- receptor knockout mice are protected against dopaminergic neurotoxicity induced by methamphetamine or MDMA. Neurobiol. Dis. 42, 391–403. https://doi.org/10.1016/j.nbd.2011.01.033.
Granado, N., Lastres-Becker, I., Ares-Santos, S., Oliva, I., Martin, E., Cuadrado, A., Moratalla, R., 2011b. Nrf2 deficiency potentiates methamphetamine-induced dopaminergic axonal damage and gliosis in the striatum. Glia 59, 1850–1863. https://doi.org/10.1002/glia.21229.
Guigoni, C., Aubert, I., Li, Q., Gurevich, V.V., Benovic, J.L., Ferry, S., Mach, U., Stark, H., Leriche, L., Håkansson, K., Bioulac, B.H., Gross, C.E., Sokolof, P., Fisone, G., Gurevich, E.V., Bloch, B., Bezard, E., 2005. Pathogenesis of levodopa-induced dyskinesia: focus on D1 and D3 dopamine receptors. Parkinsonism Relat. Disord. 11 (Suppl 1), S25–S29. https://doi.org/10.1016/j.parkreldis.2004.11.005.
Guigoni, C., Doudnikoff, E., Li, Q., Bloch, B., Bezard, E., 2007. Altered D(1) dopamine receptor trafficking in parkinsonian and dyskinetic non-human primates. Neurobiol. Dis. 26, 452–463. https://doi.org/10.1016/j.nbd.2007.02.001.
Hardy, J., Cai, H., Cookson, M.R., Gwinn-Hardy, K., Singleton, A., 2006. Genetics of Parkinson's disease and parkinsonism. Ann. Neurol. 60, 389–398. https://doi.org/10.1002/ana.21022.
Herrera, F., Outeiro, T.F., 2012. α-Synuclein modifies huntingtin aggregation in living cells. FEBS Lett. 586, 7–12. https://doi.org/10.1016/j.febslet.2011.11.019.
Hirata, H., Cadet, J.L., 1997. p53-knockout mice are protected against the long-term effects of methaphetamine on dopaminergic terminals and cell bodies. J. Neurochem. 69, 780–790. https://doi.org/10.1046/j.1471-4159.1997.69020780.x.
Iacovelli, L., Fulceri, F., De Blasi, A., Nicoletti, F., Ruggieri, S., Fornai, F., 2006. The neurotoxicity of amphetamines: bridging drugs of abuse and neurodegenerative disorders. Exp. Neurol. 201, 24–31. https://doi.org/10.1016/j.expneurol.2006.02.130.
Irvine, G.B., El-Agnaf, O.M., Shankar, G.M., Walsh, D.M., 2008. Protein aggregation in the brain: the molecular basis for Alzheimer's and Parkinson's diseases. Mol. Med. 14, 451–464. https://doi.org/10.2119/2007-00100.Irvine.
Iseki, E., Marui, W., Akiyama, H., Uéda, K., Kosaka, K., 2000. Degeneration process of Lewy bodies in the brains of patients with dementia with Lewy bodies using alpha-synuclein-immunohistochemistry. Neurosci. Lett. 286, 69–73. https://doi.org/10.1016/S0304-3940(00)01090-9.

Jakel, R.J., Maragos, W.F., 2000. Neuronal cell death in Huntington's disease: a potential role for dopamine. Trends Neurosci. 23, 239–245. https://doi.org/10.1016/S0166-2236(00)01568-X.

Jiang, W., Li, J., Zhang, Z., Wang, H., Wang, Z., 2014. Epigenetic upregulation of alpha-synuclein in the rats exposed to methamphetamine. Eur. J. Pharmacol. 745, 243–248. https://doi.org/10.1016/j.ejphar.2014.10.043.

Kiely, A.P., Ling, H., Asi, Y.T., Kara, E., Proukakis, C., Schapira, A.H., Morris, H.R., Roberts, H.C., Lubbe, S., Limousin, P., Lewis, P.A., Lees, A.J., Quinn, N., Hardy, J., Love, S., Revesz, T., Houlden, H., Holton, J.L., 2015. Distinct clinical and neuropathological features of G51D SNCA mutation cases compared with SNCA duplication and H50Q mutation. Mol. Neurodegener. 10, 41. https://doi.org/10.1186/s13024-015-0038-3.

Koros, C., Simitsi, A., Stefanis, L., 2017. Genetics of Parkinson's disease: genotype-phenotype correlations. Int. Rev. Neurobiol. 132, 197–231. https://doi.org/10.1016/bs.irn.2017.01.009.

Kousik, S.M., Carvey, P.M., Napier, T.C., 2014. Methamphetamine self-administration results in persistent dopaminergic pathology: implications for Parkinson's disease risk and reward-seeking. Eur. J. Neurosci. 40, 2707–2714. https://doi.org/10.1111/ejn.12628.

Kowall, N.W., Hantraye, P., Brouillet, E., Beal, M.F., McKee, A.C., Ferrante, R.J., 2000. MPTP induces alpha-synuclein aggregation in the substantia nigra of baboons. Neuroreport 11, 211–213.

Lazzeri, G., Lenzi, P., Busceti, C.L., Ferrucci, M., Falleni, A., Bruno, V., Paparelli, A., Fornai, F., 2007. Mechanisms involved in the formation of dopamine-induced intracellular bodies within striatal neurons. J. Neurochem. 101, 1414–1427. https://doi.org/10.1111/j.1471-4159.2006.04429.x.

Lee, S.J., Desplats, P., Sigurdson, C., Tsigelny, I., Masliah, E., 2010. Cell-to-cell transmission of non-prion protein aggregates. Nat. Rev. Neurol. 6, 702–706. https://doi.org/10.1038/nrneurol.2010.145.

Lenzi, P., Lazzeri, G., Biagioni, F., Busceti, C.L., Gambardella, S., Salvetti, A., Fornai, F., 2016. The autophagoproteasome a novel cell clearing organelle in baseline and stimulated conditions. Front. Neuroanat. 10, 78. https://doi.org/10.3389/fnana.2016.00078.

Li, X., Rubio, F.J., Zeric, T., Bossert, J.M., Kambhampati, S., Cates, H.M., Kennedy, P.J., Liu, Q.R., Cimbro, R., Hope, B.T., Nestler, E.J., Shaham, Y., 2015. Incubation of methamphetamine craving is associated with selective increases in expression of Bdnf and trkb, glutamate receptors, and epigenetic enzymes in cue-activated fos-expressing dorsal striatal neurons. J. Neurosci. 35, 8232–8244. https://doi.org/10.1523/JNEUROSCI.1022-15.2015.

Limanaqi, F., Gambardella, S., Biagioni, F., Busceti, C.L., Fornai, F., 2018. Epigenetic effects induced by methamphetamine and methamphetamine-dependent oxidative stress. Oxid. Med. Cell. Longev. 2018, 4982453. https://doi.org/10.1155/2018/4982453.

Lucocq, J.M., Habermann, A., Watt, S., Backer, J.M., Mayhew, T.M., Griffiths, G., 2004. A rapid method for assessing the distribution of gold labeling on thin sections. J. Histochem. Cytochem. 52, 991–1000. https://doi.org/10.1369/jhc.3A6178.2004.

Massart, R., Barnea, R., Dikshtein, Y., Suderman, M., Meir, O., Hallett, M., Kennedy, P., Nestler, E.J., Szyf, M., Yadid, G., 2015. Role of DNA methylation in the nucleus accumbens in incubation of cocaine craving. J. Neurosci. 35, 8042–8058. https://doi.org/10.1523/JNEUROSCI.3053-14.2015.

Matsumoto, L., Takuma, H., Tamaoka, A., Kurisaki, H., Date, H., Tsuji, S., Iwata, A., 2010. CpG demethylation enhances alpha-synuclein expression and affects the pathogenesis of Parkinson's disease. PLoS One 5, e15522. https://doi.org/10.1371/journal.pone.0015522.

McConnell, S.E., O'Banion, M.K., Cory-Slechta, D.A., Olschowka, J.A., Opanashuk, L.A., 2015. Characterization of binge-dosed methamphetamine-induced neurotoxicity and neuroinflammation. Neurotoxicology 50, 131–141. https://doi.org/10.1016/j.neuro.2015.08.006.

McCormack, A.L., Di Monte, D.A., 2009. Enhanced alpha-synuclein expression in human neurodegenerative diseases: pathogenetic and therapeutic implications. Curr. Protein. Pept. Sci. 10, 476–482. https://doi.org/10.2174/138920309789351912.

McCormack, A.L., Mak, S.K., Shenasa, M., Langston, W.J., Forno, L.S., Di Monte, D.A., 2008. Pathologic modifications of alpha-synuclein in 1-methyl-4-phenyl-1,2,3,6-tetrahydropyridine (MPTP)-treated squirrel monkeys. J. Neuropathol. Exp. Neurol. 67, 793–802. https://doi.org/10.1097/NEN.0b013e318180f0bd.

Melki, R., 2018. Alpha-synuclein and the prion hypothesis in Parkinson's disease. Rev. Neurol. (Paris) 174, 644–652. https://doi.org/10.1016/j.neurol.2018.08.002.

Mizuno, Y., Hattori, N., Kubo, S., Sato, S., Nishioka, K., Hatano, T., Tomiyama, H., Funayama, M., Machida, Y., Mochizuki, H., 2008. Progress in the pathogenesis and genetics of Parkinson's disease. Philos. Trans. R. Soc. Lond. B. Biol. Sci. 363, 2215–2227. https://doi.org/10.1098/rstb.2008.2273.

Mohn, F., Weber, M., Schübeler, D., Roloff, T.C., 2009. Methylated DNA immunoprecipitation (MeDIP). Methods Mol. Biol. 507, 55–64. https://doi.org/10.1007/978-1-59745-522-0_5.

Moratalla, R., Khairnar, A., Simola, N., Granado, N., García-Montes, J.R., Porceddu, P.F., Tizabi, Y., Costa, G., Morelli, M., 2017. Amphetamine-related drugs neurotoxicity in humans and in experimental animals: Main mechanisms. Prog. Neurobiol. 155, 149–170. https://doi.org/10.1016/j.pneurobio.2015.09.011.

Mulcahy, P., O'Doherty, A., Paucard, A., O'Brien, T., Kirik, D., Dowd, E., 2012. Development and characterisation of a novel rat model of Parkinson's disease induced by sequential intranigral administration of AAV-α-synuclein and the pesticide, rotenone. Neuroscience 17, 170–179. https://doi.org/10.1016/j.neuroscience.2011.12.011.

Novello, S., Arcuri, L., Dovero, S., Dutheil, N., Shimshek, D.R., Bezard, E., Morari, M., 2018. G2019S LRRK2 mutation facilitates α-synuclein neuropathology in aged mice. Neurobiol. Dis. 120, 21–33. https://doi.org/10.1016/j.nbd.2018.08.018.

Nussbaum, R.L., Polymeropoulos, M.H., 1997. Genetics of Parkinson's disease. Hum. Mol. Genet. 6, 1687–1691 PMID: 9300660.

O'Dell, S.J., Galvez, B.A., Ball, A.J., Marshall, J.F., 2012. Running wheel exercise ameliorates methamphetamine-induced damage to dopamine and serotonin terminals. Synapse 66, 71–80. https://doi.org/10.1002/syn.20989.

Olanow, C.W., Prusiner, S.B., 2009. Is Parkinson's disease a prion disorder? Proc. Natl. Acad. Sci. U.S.A. 106, 12571–12572. https://doi.org/10.1073/pnas.0906759106.

Omonijo, O., Wongprayoon, P., Ladenheim, B., McCoy, M.T., Govitrapong, P., Jayanthi, S., Cadet, J.L., 2014. Differential effects of binge methamphetamine injections on the mRNA expression of histone deacetylases (HDACs) in the rat striatum. Neurotoxicology 45, 178–184. https://doi.org/10.1016/j.neuro.2014.10.008.

Poças, G.M., Branco-Santos, J., Herrera, F., Outeiro, T.F., Domingos, P.M., 2015. α-Synuclein modifies mutant huntingtin aggregation and neurotoxicity in Drosophila. Hum. Mol. Genet. 24, 1898–1907. https://doi.org/10.1093/hmg/ddu606.

Preston, K.L., Wagner, G.C., Schuster, C.R., Seiden, L.S., 1985. Long-term effects of repeated methylamphetamine administration on monoamine neurons in the rhesus monkey brain. Brain Res. 338, 243–248. https://doi.org/10.1016/0006-8993(85)90153-2.

Purisai, M.G., McCormack, A.L., Langston, W.J., Johnston, L.C., Di Monte, D.A., 2005. Alpha-synuclein expression in the substantia nigra of MPTP-lesioned non-human primates. Neurobiol. Dis. 20, 898–906. https://doi.org/10.1016/j.nbd.2005.05.028.

Reichenbach, N., Herrmann, U., Kähne, T., Schicknick, H., Pielot, R., Naumann, M., Dieterich, D.C., Gundelfinger, E.D., Smalla, K.H., Tischmeyer, W., 2015. Differential effects of dopamine signalling on long-term memory formation and consolidation in rodent brain. Proteome Sci. 13 (13), 2015. https://doi.org/10.1186/s12953-015-0069-2. eCollection.

Renthal, W., Nestler, E.J., 2008. Epigenetic mechanisms in drug addiction. Trends Mol. Med. 14, 341–350. https://doi.org/10.1016/j.molmed.2008.06.004.

Ricaurte, G.A., Schuster, C.R., Seiden, L.S., 1980. Long-term effects of repeated methylamphetamine administration on dopamine and serotonin neurons in the rat brain: a regional study. Brain Res. 193, 153–163. https://doi.org/10.1016/0006-8993(80)90952-X.

Ricaurte, G.A., Guillery, R.W., Seiden, L.S., Schuster, C.R., Moore, R.Y., 1982. Dopamine nerve terminal degeneration produced by high doses of methylamphetamine in the rat brain. Brain Res. 235, 93–103. https://doi.org/10.1016/0006-8993(82)90198-6.

Ricaurte, G.A., Seiden, L.S., Schuster, C.R., 1984. Further evidence that amphetamines produce long-lasting dopamine neurochemical deficits by destroying dopamine nerve fibers. Brain Res. 303, 359–364. https://doi.org/10.1016/0006-8993(84)91221-6.

Robison, A.J., Nestler, E.J., 2011. Transcriptional and epigenetic mechanisms of addiction. Nat. Rev. Neurosci. 12, 623–637. https://doi.org/10.1038/nrn3111.

Schlüter, O.M., Fornai, F., Alessandrí, M.G., Takamori, S., Geppert, M., Jahn, R., Südhof, T.C., 2003. Role of alpha-synuclein in 1-methyl-4-phenyl-1,2,3,6-tetrahydropyridine-induced parkinsonism in mice. Neuroscience 118, 985–1002. https://doi.org/10.1016/S0306-4522(03)00036-8.

Schmidt, C.J., Ritter, J.K., Sonsalla, P.K., Hanson, G.R., Gibb, J.W., 1985. Role of dopamine in the neurotoxic effects of methamphetamine. J. Pharmacol. Exp. Ther. 233, 539–544 PMID: 2409267.

Seiden, L.S., 1985. Methamphetamine: toxicity to dopaminergic neurons. NIDA Res. Monogr. 62, 100–106 PMID: 2867472.

Seiden, L.S., Fischman, M.W., Schuster, C.R., 1976. Long-term methamphetamine induced changes in brain catecholamines in tolerant rhesus monkeys. Drug Alcohol Depend. 1, 215–219. https://doi.org/10.1016/0376-8716(76)90030-2.

Singleton, A.B., Farrer, M., Johnson, J., Singleton, A., Hague, S., Kachergus, J., Hulihan, M., Peuralinna, T., Dutra, A., Nussbaum, R., Lincoln, S., Crawley, A., Hanson, M., Maraganore, D., Adler, C., Cookson, M.R., Muenter, M., Baptista, M., Miller, D., Blancato, J., Hardy, J., Gwinn-Hardy, K., 2003. alpha-Synuclein locus triplication causes Parkinson's disease. Science 302, 841. https://doi.org/10.1126/science.1090278.

Singleton, A.B., Farrer, M.J., Bonifati, V., 2013. The genetics of Parkinson's disease: progress and therapeutic implications. Mov. Disord. 28, 14–23. https://doi.org/10.1002/mds.25249.

Smith, G.A., Breger, L.S., Lane, E.L., Dunnett, S.B., 2012. Pharmacological modulation of amphetamine-induced dyskinesia in transplanted hemi-parkinsonian rats. Neuropharmacology 63, 818–828. https://doi.org/10.1016/j.neuropharm.2012.06.011.

Sonsalla, P.K., Jochnowitz, N.D., Zeevalk, G.D., Oostveen, J.A., Hall, E.D., 1996. Treatment of mice with methamphetamine produces cell loss in the substantia nigra. Brain Res. 738, 172–175.

Spacey, S.D., Wood, N.W., 1999. The genetics of Parkinson's disease. Curr. Opin. Neurol. 12, 427–432 PMID: 10555831.

Spillantini, M.G., Crowther, R.A., Jakes, R., Hasegawa, M., Goedert, M., 1998. alpha-Synuclein in filamentous inclusions of Lewy bodies from Parkinson's disease and dementia with lewy bodies. Proc. Natl. Acad. Sci. U.S.A. 95, 6469–6473. https://doi.org/10.1073/pnas.95.11.6469.

Stone, D.M., Johnson, M., Hanson, G.R., Gibb, J.W., 1988. Role of endogenous dopamine in the central serotonergic deficits induced by 3,4-methylenedioxymethamphetamine. J. Pharmacol. Exp. Ther. 247, 79–87 PMID: 2902215.

Thakur, P., Breger, L.S., Lundblad, M., Wan, O.W., Mattsson, B., Luk, K.C., Lee, V.M.Y., Trojanowski, J.Q., Björklund, A., 2017. Modeling Parkinson's disease pathology by combination of fibril seeds and α-synuclein overexpression in the rat brain. Proc. Natl. Acad. Sci. U.S.A. 114, E8284–E8293. https://doi.org/10.1073/pnas.1710442114.

Tomás-Zapico, C., Díez-Zaera, M., Ferrer, I., Gómez-Ramos, P., Morán, M.A., Miras-Portugal, M.T., Díaz-Hernández, M., Lucas, J.J., 2012. α-Synuclein accumulates in huntingtin inclusions but forms independent filaments and its deficiency attenuates early phenotype in a mouse model of Huntington's disease. Hum. Mol. Genet. 21,

495–510. https://doi.org/10.1093/hmg/ddr507.
Totterdell, S., Hanger, D., Meredith, G.E., 2004. The ultrastructural distribution of alpha-synuclein-like protein in normal mouse brain. Brain Res. 1004, 61–72. https://doi.org/10.1016/j.brainres.2003.10.072.
Vance, J.M., Ali, S., Bradley, W.G., Singer, C., Di Monte, D.A., 2010. Gene-environment interactions in Parkinson's disease and other forms of parkinsonism. Neurotoxicology 31, 598–602. https://doi.org/10.1016/j.neuro.2010.04.007.
Villemagne, V.L., Wong, D.F., Yokoi, F., Stephane, M., Rice, K.C., Matecka, D., Clough, D.J., Dannals, R.F., Rothman, R.B., 1999. GBR12909 attenuates amphetamine-induced striatal dopamine release as measured by [(11)C]raclopride continuous infusion PET scans. Synapse 33, 268–273. https://doi.org/10.1002/(SICI)1098-2396(19990915)33:4<268::AID-SYN3>3.0.CO;2-W.
Villemagne, V., Yuan, J., Wong, D.F., Dannals, R.F., Hatzidimitriou, G., Mathews, W.B., Ravert, H.T., Musachio, J., McCann, U.D., Ricaurte, G.A., 1998. Brain dopamine neurotoxicity in baboons treated with doses of methamphetamine comparable to those recreationally abused by humans: evidence from [11C] WIN-35,428 positron emission tomography studies and direct in vitro determinations. J. Neurosci. 18, 419–427. https://doi.org/10.1523/JNEUROSCI.18-01-00419.1998.
Volkow, N.D., Chang, L., Wang, G.J., Fowler, J.S., Franceschi, D., Sedler, M., Gatley, S.J., Miller, E., Hitzemann, R., Ding, Y.S., Logan, J., 2001. Loss of dopamine transporters in methamphetamine abusers recovers with protracted abstinence. J. Neurosci. 21, 9414–9418. https://doi.org/10.1523/JNEUROSCI.21-23-09414.2001.
Wagner, G.C., Seiden, L.S., Schuster, C.R., 1979. Methamphetamine-induced changes in brain catecholamines in rats and guinea pigs. Drug Alcohol Depend. 4, 435–438. https://doi.org/10.1016/0376-8716(79)90076-0.
Wagner, G.C., Ricaurte, G.A., Seiden, L.S., Schuster, C.R., Miller, R.J., Westley, J., 1980a. Long-lasting depletions of striatal dopamine and loss of dopamine uptake sites following repeated administration of methamphetamine. Brain Res. 181, 151–160. https://doi.org/10.1016/0006-8993(80)91265-2. a.
Wagner, G.C., Lucot, J.B., Schuster, C.R., Seiden, L.S., 1983. Alpha-methyltyrosine attenuates and reserpine increases methamphetamine-induced neuronal changes. Brain Res. 270, 285–288. https://doi.org/10.1016/0006-8993(83)90602-9.
Wagner, C., Ricaurte, G.A., Johanson, C.E., Schuster, C.R., Seiden, L.S., 1980b. Amphetamine induces depletion of dopamine and loss of dopamine uptake sites in caudate. Neurology 30, 547–550 PMID: 6768005 b.
Walker, D.M., Nestler, E.J., 2018. Neuroepigenetics and addiction. Handb. Clin. Neurol. 148, 747–765. https://doi.org/10.1016/B978-0-444-64076-5.00048-X.
Wong, Y.C., Krainc, D., 2017. α-synuclein toxicity in neurodegeneration: mechanism and therapeutic strategies. Nat. Med. 23, 1–13. https://doi.org/10.1038/nm.4269.
Woolverton, W.L., Ricaurte, G.A., Forno, L.S., Seiden, L.S., 1989. Long-term effects of chronic methamphetamine administration in rhesus monkeys. Brain Res. 486, 73–78. https://doi.org/10.1016/0006-8993(89)91279-1.
Zhu, J.P., Xu, W., Angulo, N., Angulo, J.A., 2006. Methamphetamine-induced striatal apoptosis in the mouse brain: comparison of a binge to an acute bolus drug administration. Neurotoxicology 27, 131–136. https://doi.org/10.1016/j.neuro.2005.05.014.